J|A|C|S
ARTICLES
Published on Web 06/18/2002

Photoaffinity Analogues of Farnesyl Pyrophosphate Transferable by Protein Farnesyl Transferase

Kareem A. H. Chehade,[†,§] Katarzyna Kiegiel,[†,§] Richard J. Isaacs,[†,§] Jennifer S. Pickett,[||] Katherine E. Bowers,[||] Carol A. Fierke,[||] Douglas A. Andres,[†,§] and H. Peter Spielmann*[,†,‡,§]

Contribution from the Department of Molecular and Cellular Biochemistry, Department of Chemistry, Kentucky Center for Structural Biology, University of Kentucky, Lexington, Kentucky 40536-0084, and Department of Chemistry, University of Michigan, Ann Arbor, Michigan 48109

Received November 5, 2001

Abstract: Farnesylation is a posttranslational lipid modification in which a 15-carbon farnesyl isoprenoid is linked via a thioether bond to specific cysteine residues of proteins in a reaction catalyzed by protein farnesyltransferase (FTase). We synthesized analogues (**3**−**6**) of farnesyl pyrophosphate (FPP) to probe the range of modifications possible to the FPP skeleton which allow for efficient transfer by FTase. Photoaffinity analogues of FPP (**5**, **6**) were prepared by substituting perfluorophenyl azide functional groups for the ω-terminal isoprene of FPP. Substituted anilines replace the ω-terminal isoprene in analogues **3** and **4**. Compounds **3**−**5** were prepared by reductive amination of the appropriate anilines with 8-oxo-geranyl acetate, followed by ester hydrolysis, chlorination, and pyrophosphorylation. Additional substitution of three methylenes for the β-isoprene of FPP gave photoprobe **6** in nine steps. Preparation of the analogues required $TiCl_4$-mediated imine formation prior to $NaBH(OAc)_3$ reduction for anilines with a $pK_a < 1$. The azide moiety was not affected by Ph_3PCl_2 conversion of allylic alcohols **13**−**16** into corresponding chlorides **17**−**20**. Analogues **3**−**6** are efficiently transferred to target *N*-dansyl-GCVLS peptide substrate by mammalian FTase. Comparison of analogue structures and kinetics of transfer to those of FPP reveals that ring fluorination and para substituents have little effect on the affinity of the analogue pyrophosphate for FTase and its transfer efficiency. These results are also supported with models of the analogue binding modes in the active site of FTase. The transferable azide photoprobe **5** photoinactivates FTase. Transferable analogues **5** and **6** allow the formation of appropriately posttranslationally modified photoreactive peptide probes of isoprene function.

The Ras family of proteins play a pivotal role in the control of cellular growth and differentiation through their interaction with a variety of cellular effectors. Ras is a monomeric GTPase which is associated with the inner leaflet of the plasma membrane and functions as a binary molecular switch that cycles between inactive GDP and active GTP bound states.[1] Posttranslational modification of Ras with the 15-carbon farnesyl isoprenoid is essential for the protein to become properly localized to the inner leaflet of the plasma membrane.[2−4] Protein farnesyltransferase (FTase) catalyzes the formation of a thioether between the farnesyl isoprenoid from farnesyl pyrophosphate **1** (FPP) and a conserved cysteine in protein substrates.[2,5] The reactive cysteine is located in the C-terminal Ca_1a_2X motif in which C is the cysteine to be modified, a_1 and a_2 are often aliphatic residues, and X is one of various residues including Ser, Met, Ala, or Gln.[2] Mutated forms of cellular Ras genes are among the most common genetic abnormalities in human cancer, occurring in 30% of all neoplasms.[6−11] Furthermore, farnesylation of Ras is required to transform cells.[7,12,13] Consequently, a number of selective FTase inhibitors (FTIs) that prevent Ras farnesylation have been developed as anticancer therapeutics.[14−21]

* To whom correspondence should be addressed. Telephone: 859-257-4790. Fax: 859-257-8940. E-mail: hps@pop.uky.edu.
[†] Department of Molecular and Cellular Biochemistry, University of Kentucky.
[‡] Department of Chemistry, University of Kentucky.
[§] Kentucky Center for Structural Biology, University of Kentucky.
[||] University of Michigan.

(1) Scheffzek, K.; Ahmadian, M. R.; Wittinghofer, A. *Trends Biochem. Sci.* **1998**, *23*, 257.
(2) Zhang, F. L.; Casey, P. J. *Annu. Rev. Biochem.* **1996**, *65*, 241−269.
(3) Reiss, Y.; Goldstein, J. L.; Seabra, M. C.; Casey, P. J.; Brown, M. S. *Cell* **1990**, *62*, 81−88.
(4) Glomset, J. A.; Farnsworth, C. C. *Annu. Rev. Cell Biol.* **1994**, *10*, 181−205.
(5) Hightower, K. E.; Fierke, C. A. *Curr. Opin. Chem. Biol.* **1998**, *3*, 176.
(6) Casey, P. J.; Solski, P. A.; Der, C. J.; Buss, J. E. *Proc. Natl. Acad. Sci. U.S.A.* **1989**, *86*, 8323−8327.
(7) Hancock, J. F.; Magee, A. I.; Childs, J. E.; Marshall, C. J. *Cell* **1989**, *57*, 1167−1177.
(8) Schafer, W. R.; Kim, R.; Sterne, R.; Thorner, J.; Kim, S. H.; Rine, J. *Science* **1989**, *245*, 379−385.
(9) Bos, J. L. *Cancer Res.* **1989**, *49*, 4682−4689.
(10) Clark, G. J.; Der, C. J. *Ras Proto-oncogene Activation in Human Malignancy*; Humana Press: Totowa, NJ, 1995; pp 17−52.
(11) Khosravi-Far, R.; Der, C. J. *Cancer Metastasis Rev.* **1994**, *13*, 67−89.
(12) Schafer, W. R.; Rine, J. *Annu. Rev. Genet.* **1992**, *30*, 209−237.
(13) Barbacid, M. *Annu. Rev. Biochem.* **1987**, *56*, 779−827.
(14) Gibbs, J. B.; Oliff, A. *Annu. Rev. Pharmacol. Toxicol.* **1997**, *37*, 143−166.

10.1021/ja0124717 CCC: $22.00

Although our understanding of the biological consequences of Ras farnesylation has increased significantly in recent years, there is relatively little known about the molecular details of the interactions that give rise to the lipid's functional role and of the processes downstream of farnesylation. Major questions such as whether the lipid participates in protein−protein recognition or the exact mechanism by which the modified Ras is directed only to the inner leaflet of the plasma membrane remain unanswered. While farnesylation of Ras is absolutely required for its biological effects and membrane localization, it is unclear whether the prenyl group functions as a hydrophobic membrane association signal,[7,22−26] a protein recognition signal, or both.[27,28] Recently, several X-ray crystal structures of the Ras related small G-proteins Rac and Cdc42 in complex with the GDP dissociation inhibitor protein RhoGDI have become available. In contrast to Ras, Rac and Cdc42 are geranylgeranylated and are cytosolically located in a complex with RhoGDI in resting cells. The X-ray crystal structures of the complexes show that the geranylgeranyl group is completely inserted into a hydrophobic binding pocket of RhoGDI.[29−31]

Heterobifunctional photoprobe analogues of farnesyl pyrophosphate that are transferred by FTase to Ras should enable the dissection of these interactions through the identification of specific molecular partners. Analogues of FPP that are alternative transferable substrates for FTase have been utilized to study farnesylation and some aspects of the subsequent downstream processing events.[26,32−37] FPP analogues stripped of most isoprenoid features such as methyl groups and unsaturation to more closely resemble simple fatty acids are transferred to Ras by FTase and allow Ras to function in a *Xenopus* signal transduction model system.[26] Photoaffinity labeling has been used extensively in the study of protein structure and function,[38,39] and photoaffinity analogues of FPP derivatized with diazoketone and benzophenone photoaffinity moieties have been synthesized.[40−51] Unfortunately, none of the FPP photoaffinity analogues described in the literature are efficiently transferred by FTase to protein substrates.[40−50] A significant impediment to the development of heterobifunctional FPP photoprobes is that the FTase-catalyzed transfer of analogues to substrate is very sensitive to the structure of the lipid.[26,36,37,40−50] FPP analogues containing diazoketone functionality are not transferred by FTase and instead act as FTIs.[40−44] The best transferable FPP photoaffinity probe developed to date is derived from an ether linked benzophenone moiety in place of the β- and ω-isoprene units of FPP.[50] This analogue is transferred to protein substrate very slowly with low efficiency and requires prolonged UV irradiation to photochemically inactivate yeast FTase. Recently, the isoprenoid portion of this analogue S-linked to cysteine has been employed as a photoprobe of the isoprenoid binding protein RhoGDI.[49]

Substitution of the terminal isoprene of FPP by an aniline group gives 8-anilinogeranyl pyrophosphate (**2**, AGPP, Figure 1), which is transferred to Ras by FTase with the same kinetics as FPP.[36] Transferable FPP analogues **38**−**42** were also obtained by replacing the ω-isoprene of FPP with a benzyloxy group and substitution of the β-isoprene with a variable length methylene chain (Figure 2).[37] These studies indicate that an aromatic ring is an acceptable isostere for the terminal isoprene of FPP in the FTase-catalyzed transfer of lipid to substrate. Consequently, transferable FPP photoprobes based on perfluorophenyl azides are an attractive alternative to diazoketone and benzophenone photoaffinity reagents because they have different steric and electronic properties.

We report the synthesis and biochemical characterization of FPP analogues **3** and **4** which contain substituted anilines and of the heterobifunctional perfluorophenyl azide FPP photoanalogues **5** and **6**. Pyrophosphates **3**−**6** are transferred by FTase to dansyl-GCVLS peptide substrate, and analogue **5** inactivates FTase in a light-dependent manner. Comparison of the analogue structures and kinetics of analogue transfer with those of FPP reveal that ring fluorination and para substituents have little effect on the affinity of the analogue pyrophosphate for FTase and its transfer efficiency. These results are also supported with models of the analogue binding modes in the active site of FTase. Additionally, we have found that weakly basic anilines having a $pK_a \geq 1$ are successfully alkylated by standard reductive amination conditions, while alkylation of anilines

(15) Leonard, D. M. *J. Med. Chem.* **1997**, *40*, 2971−2990.
(16) Sebti, S. M.; Hamilton, A. D. *Pharmacol. Ther.* **1997**, *74*, 103−114.
(17) Rowinsky, E. K.; Windle, J. J.; Von Hoff, D. D. *J. Clin. Oncol.* **1999**, *17*, 3631−3652.
(18) Sebti, S. M.; Hamilton, A. D. *Expert Opin. Invest. Drugs* **2000**, *9*, 2767−2782.
(19) Prendergast, G. C.; Rane, N. *Expert Opin. Invest. Drugs* **2001**, *10*, 2105−16.
(20) Singh, S. B.; Lingham, R. B. *Curr. Opin. Drug Discovery Dev.* **2002**, *5*, 225−44.
(21) Ganguly, A. K.; Doll, R. J.; Girijavallabhan, V. M. *Curr. Med. Chem.* **2001**, *8*, 1419−36.
(22) Hancock, J. F.; Cadwallader, K.; Paterson, H.; Marshall, C. J. *EMBO J.* **1991**, *10*, 4033−4039.
(23) Hancock, J. F.; Cadwallader, K.; Marshall, C. J. *EMBO J.* **1991**, *10*, 641−646.
(24) Leevers, S. J.; Paterson, H. F.; Marshall, C. J. *Nature* **1994**, *369*, 411−414.
(25) Stokoe, D.; Macdonald, S. G.; Cadwallader, K.; Symons, M.; Hancock, J. F. *Science* **1994**, *264*, 1463−1467.
(26) Dudler, T.; Gelb, M. H. *Biochemistry* **1997**, *36*, 12434−12441.
(27) Marshall, C. J. *Science* **1993**, *259*, 1865−1866.
(28) Casey, P. J. *Science* **1995**, *268*, 221−225.
(29) Grizot, S.; Faure, J.; Fieschi, F.; Vignais, P. V.; Dagher, M. C.; Pebay-Peyroula, E. *Biochemistry* **2001**, *40*, 10007−13.
(30) Hoffman, G. R.; Nassar, N.; Cerione, R. A. *Cell* **2000**, *100*, 345−56.
(31) Scheffzek, K.; Stephan, I.; Jensen, O. N.; Illenberger, D.; Gierschik, P. *Nat. Struct. Biol.* **2000**, *7*, 122−6.
(32) Gibbs, R. A.; Krishnan, U.; Dolence, J. M.; Poulter, C. D. *J. Org. Chem.* **1995**, *60*, 7821.
(33) Mu, Y. Q.; Gibbs, R. A.; Eubanks, L. M.; Poulter, C. D. *J. Org. Chem.* **1996**, *61*, 8010.
(34) Shao, Y.; Eummer, J. T.; Gibbs, R. A. *Org. Lett.* **1999**, *1*, 627−630.
(35) Gibbs, B. S.; Zahn, T. J.; Mu, Y. Q.; Sebolt-Leopold, J. S.; Gibbs, R. A. *J. Med. Chem.* **1999**, *42*, 3800.
(36) Chehade, K. A. H.; Andres, D. A.; Morimoto, H.; Spielmann, H. P. *J. Org. Chem.* **2000**, *65*, 3027−3033.
(37) Micali, E.; Chehade, K. A.; Isaacs, R. J.; Andres, D. A.; Spielmann, H. P. *Biochemistry* **2001**, *40*, 12254−65.
(38) Bayley, H. *Photogenerated Reagents in Biochemistry and Molecular Biology*; Elsevier: New York, 1983.
(39) Schuster, D. I.; Probst, W. C.; Ehrlich, G. K.; Singh, G. *Photochem. Photobiol.* **1989**, *49*, 785.
(40) Baba, T.; Allen, C. M. *Biochemistry* **1984**, *23*, 1312−1322.
(41) Baba, T.; Muth, J.; Allen, C. M. *J. Biol. Chem.* **1985**, *260*, 10467−10473.
(42) Allen, C. M. *Methods Enzymol.* **1985**, *110*, 117−124.
(43) Bukhtiyarov, Y. E.; Omer, C. A.; Allen, C. M. *J. Biol. Chem.* **1995**, *270*, 19035−19040.
(44) Das, N. P.; Allen, C. M. *Biochem. Biophys. Res. Commun.* **1991**, *181*, 729−735.
(45) Gaon, I.; Turek, T. C.; Weller, V. A.; Edelstein, R. L.; Singh, S. K.; Distefano, M. D. *J. Org. Chem.* **1996**, *61*, 7738−7745.
(46) Gaon, I.; Turek, T. C.; Distefano, M. D. *Tetrahedron Lett.* **1996**, *37*, 8833−8836.
(47) Turek, T. C.; Gaon, I.; Distefano, M. D. *Tetrahedron Lett.* **1996**, *37*, 4845−4848.
(48) Edelstein, R. L.; Distefano, M. D. *Biochem. Biophys. Res. Commun.* **1997**, *235*, 377−382.
(49) Kale, T. A.; Raab, C.; Yu, N.; Dean, D. C.; Distefano, M. D. *J. Am. Chem. Soc.* **2001**, *123*, 4373−4381.
(50) Turek, T. C.; Gaon, I.; Distefano, M. D. *J. Org. Chem.* **2001**, *66*, 3253−3264.
(51) Zhang, Y. W.; Koyama, T.; Marecak, D. M.; Prestwich, G. D.; Maki, Y.; Ogura, K. *Biochemistry* **1998**, *37*, 13411−20.

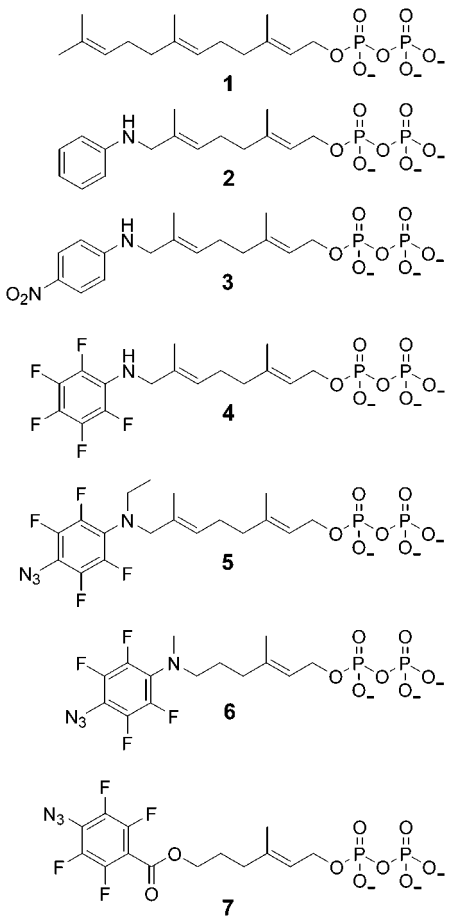

Figure 1. Structure of farnesyl pyrophosphate (**1**, FPP), 6-(4-azidotetrafluorobenzylester)-3-methyl-2-hexene pyrophosphate (**7**), and transferable FPP analogues 8-anilinogeranyl pyrophosphate (**2**, AGPP), 8-(*p*-nitroanilino)geranyl pyrophosphate (**3**, NAGPP), 8-(pentafluoroanilino)geranyl pyrophosphate (**4**, PFAGPP), 8-(*p*-azido-*N*-ethyl-tetrafluoroanilino)geranyl pyrophosphate (**5**, ETAZAGPP), and 6-(*p*-azido-*N*-methyl-tetrafluoroanilino)-3-methyl-2-hexenyl pyrophosphate (**6**, MTAZA2PP).

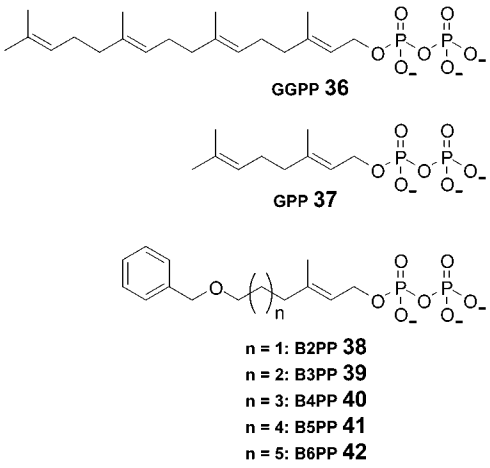

Figure 2.

having a pK_a < 1 requires imine preformation by $TiCl_4$ prior to $NaBH(OAc)_3$ reduction. The development of heterobifunctional photoprobes **5** and **6** should allow for the study of protein prenyltransferases and other enzymes that employ FPP or GGPP as their substrates. In addition, incorporation of this analogue into peptides or proteins may allow for the detection of other unknown isoprenoid binding proteins.

Results and Discussion

Design of Photoaffinity Analogues. The synthetic route outlined in Scheme 1 provides a convenient method for the incorporation of a wide variety of functionalized anilines into the 8-anilinogeranyl skeleton through reductive amination.[36] Examination of the six available FTase X-ray crystal structures with and without bound substrates suggests that transferable FPP analogues containing azide substituted aromatic groups might be accommodated in the active site of the enzyme.[50,52−56] To this end, compounds **3**−**7** (Schemes 1 and 2) were synthesized to test the range of chemical functionalities, that when incorporated into FPP analogues, would still allow appropriate transfer of lipid to protein substrate by FTase.

Synthesis of FPP Analogues 3 and 4 and Photoprobe 5. We have previously shown that acetate **9** was obtained in good yield by the addition of a slight excess of $NaBH(OAc)_3$ to a solution of aldehyde **8** and aniline in 1,2-dichloroethane at 25 °C.[36] Substitution of *p*-nitroaniline for aniline in this reaction afforded allylic amine **10** in 64% yield. However, reaction of pentafluoroaniline under these conditions only resulted in reduction of aldehyde **8** without formation of aniline **11**. We found that synthesis of allylic amine **11** required preformation of the imine intermediate prior to hydride reduction. The desired imine was formed in a few hours by condensation of aldehyde **8** with pentafluoroaniline in the presence of $TiCl_4$ and excess pyridine.[57] The perfluoro imine was isolated by column chromatography and characterized by NMR, IR, and mass spectroscopy and can be stored indefinitely at −20 °C under argon. In practice, the imine-$TiCl_4$ complex was treated in situ with a slight excess of $NaBH(OAc)_3$ and glacial acetic acid for 16 h to provide amine **11** in 60% yield after chromatography. Attempts to preform the imine with trimethylorthoformate[58] or titanium(IV) isopropoxide[59−61] failed. Formation of the imine in the presence of dehydrating agents (molecular sieves or anhydrous $CaSO_4$) or by the azeotropic removal of water required long reaction times (80 °C, 1 week) and gave very low yields.

Successful reductive amination of the pentafluoroaniline model system allowed us to proceed with the synthesis of the target heterobifunctional photoprobes. The perfluorophenyl azides were chosen as the light-activated moiety in this design because the nitrene produced upon photolysis is likely to remain in its singlet state and be more reactive toward C−H bond insertion.[62] This is important because the biologically relevant binding sites for prenyl groups are anticipated to be hydrophobic. We envisioned introduction of the azide function into the

(52) Park, H.-W.; Boduluri, S. R.; Moomaw, J. F.; Casey, P. J.; Beese, L. S. *Science* **1997**, *275*, 1800−1804.
(53) Dunten, P.; Kammlott, U.; Crowther, R.; Weber, D.; Palermo, R.; Birktoft, J. *Biochemistry* **1998**, *37*, 7907−7912.
(54) Long, S. B.; Casey, P. J.; Beese, L. S. *Biochemistry* **1998**, *37*, 9612−9618.
(55) Long, S. B.; Casey, P. J.; Beese, L. S. *Structure* **2000**, *8*, 209.
(56) Strickland, C. L.; Windsor, W. T.; Syto, R.; Wang, L.; Bond, R.; Wu, Z.; Schwartz, J.; Le, H. V.; Beese, L. S.; Weber, P. C. *Biochemistry* **1998**, *37*, 16601.
(57) Carlson, R.; Larsson, U.; Hansson, L. *Acta Chem. Scand.* **1992**, *46*, 1211−1214.
(58) Look, G. C.; Murphy, M. M.; Campbell, D. A.; Gallop, M. A. *Tetrahedron Lett.* **1995**, *36*, 2937−2940.
(59) Mattson, R. J.; Pham, K. M.; Leuck, D. J.; Cowen, K. A. *J. Org. Chem.* **1990**, *55*, 2552−2554.
(60) Bhattacharyya, S. *Tetrahedron Lett.* **1994**, *35*, 2401−2404.
(61) Bhattacharyya, S.; Chatterjee, A.; Williamson, J. S. *Synlett* **1995**, 1079−1080.
(62) Leyva, E.; Young, M. J. T.; Platz, M. S. *J. Am. Chem. Soc.* **1986**, *108*, 8307−8309.

Scheme 1 [a]

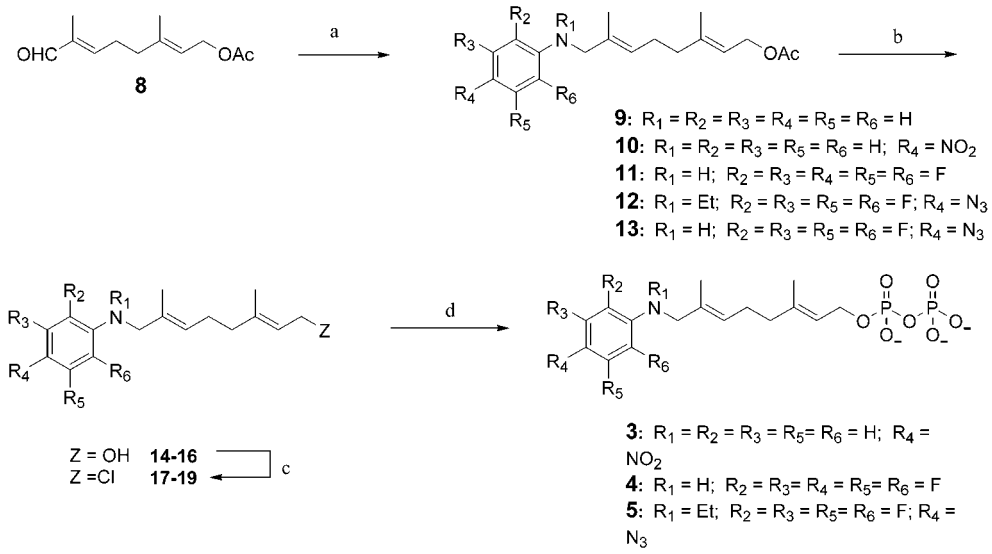

[a] Reaction conditions: (1a) *p*-nitroaniline, $NaBH(OAc)_3$, HOAc, $(CH_2Cl)_2$, or (2a) pentafluoroaniline or *p*-azidotetrafluoraniline, $TiCl_4$, $NaBH(OAc)_3$, HOAc, $(CH_2Cl)_2$; (b) K_2CO_3, H_2O, MeOH; (c) $(Ph)_3PCl_2$, Hünig's base, CH_3CN; (d) $[(n\text{-}Bu)_4N]_3HP_2O_7$, CH_3CN.

Scheme 2 [a]

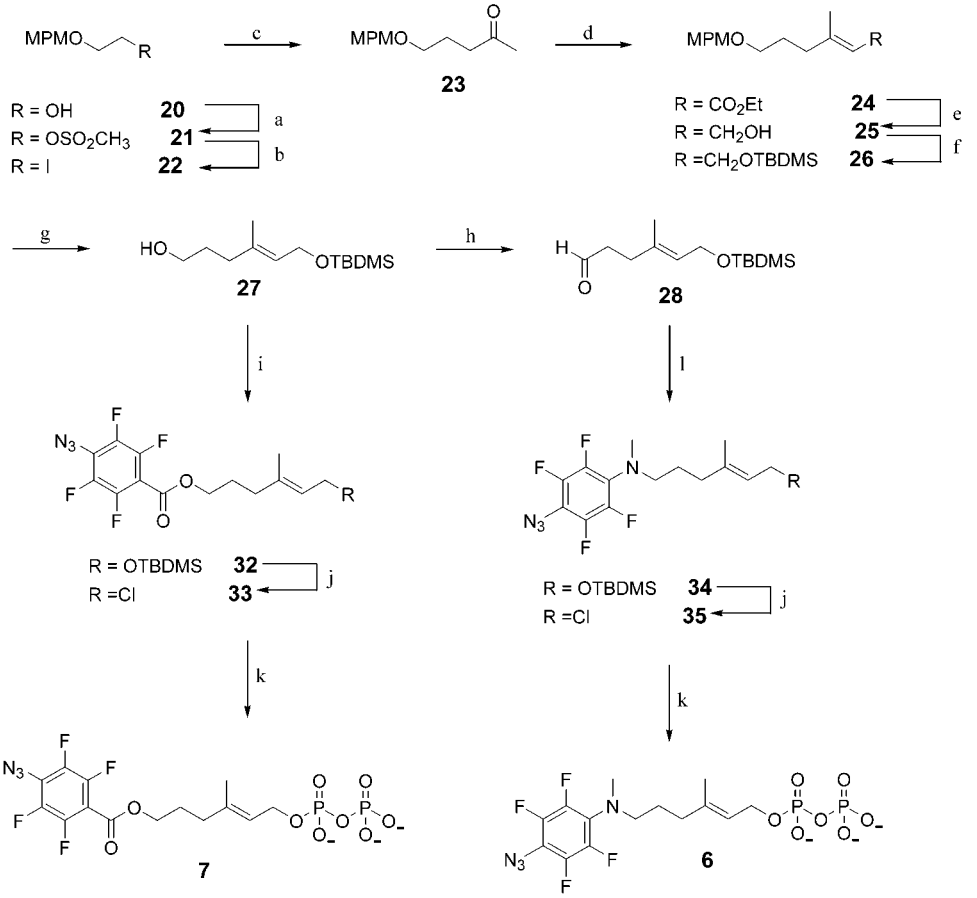

[a] Reaction conditions: (a) MsCl, pyridine; (b) NaI, acetone; (c) sodium ethylacetoacetate; (d) $(EtO)_2POCH_2CO_2Et$, NaH, THF; (e) DIBAL-H, THF; (f) TBDMS-Cl, imidazole; (g) DDQ, CH_2Cl_2/pH 7.2 buffer; (h) $(COCl)_2$, DMSO, Et_3N; (i) *p*-azidotetrafluorobenzoyl chloride, pyridine; (j) $(Ph)_3PCl_2$, CH_2Cl_2; (k) $[(n\text{-}Bu)_4N]_3HP_2O_7$, CH_3CN; (l) (1) *N*-Me-*p*-azidotetrafluoroaniline, $TiCl_4$, (2) HOAc, $NaBH(OAc)_3$.

8-anilinogeranyl backbone by reductive amination of *p*-azidotetrafluoroaniline. However, using conditions developed for pentafluoroaniline **11**, we found it was not possible to isolate pure azidoaniline **13**. Azidoaniline **13** was found to be very unstable, rapidly decomposing into deeply colored materials during attempted isolation and purification. Previously, we had shown that *p*-azidotetrafluoroaniline itself readily decomposes.[63] We reasoned that introduction of an alkyl substituent onto the aniline nitrogen would increase the stability of the desired azidoaniline. Inspection of the six crystal structures of FTase

(63) Chehade, K. A. H.; Spielmann, H. P. *J. Org. Chem.* **2000**, *65*, 4949−4953.

Scheme 3 [a]

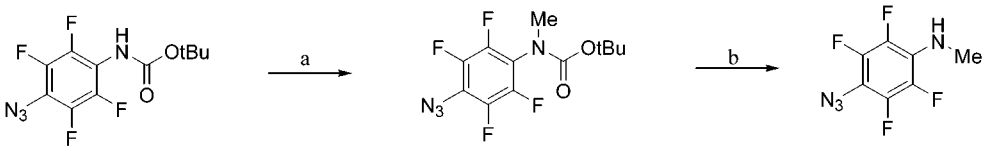

[a] Reaction conditions: (a) MeI, LHDMS, THF; (b) 1 N HCl in HOAc.

with and without bound substrates[50,52−56] suggested that small alkyl substituents on the aniline nitrogen of **13** might yield transferable analogues. Gribble and co-workers have described mild conditions for the ethylation of secondary amines in situ by alkoxy reducing agents, including $NaBH(OAc)_3$.[64,65] *N*-Ethylation of secondary amines by $NaBH(OAc)_3$ is slower than the reduction of imines, suggesting that the desired tertiary amine **12** could be obtained in one pot by modification of the conditions to form **11**. Reaction of the *p*-azidotetrafluoroaniline imine-$TiCl_4$ complex with a 3-fold excess of $NaBH(OAc)_3$ for 48 h gave *N*-ethyl azidoaniline **12** in 56% yield after chromatography. Under these conditions, no azidoaniline **13** was isolated from the reaction mixture, and, more importantly, the tertiary amine dramatically enhanced the stability of azide **12**.

Integration of the ^{1}H NMR spectrum of amines **10**−**12** indicated that a mixture of cis/trans isomers about the 6,7 double bond was formed in a 7:93 ratio. This was expected for amine **10**, because an identical cis/trans mixture was previously observed for amine **9**.[36] Interestingly, preformation of the perfluoro imines and reduction in the presence of titanium did not lead to any alteration of the cis/trans ratio for amines **11** and **12**. The cis and trans isomers of acetate **11** were easily separated by employing reverse-phase HPLC.

The allylic acetates **9**−**12** were elaborated into pyrophosphates **3**−**5** as previously described.[36] The acetates **9**−**12** were first saponified with K_2CO_3 in $MeOH/H_2O$ to generate alcohols **14**−**16**, respectively, in high yield (89−95%). Allylic alcohols **14**−**16** were converted into their corresponding chlorides **17**−**19** by dichlorotriphenylphosphorane (Ph_3PCl_2) in MeCN. Chloride **19** was obtained without any decomposition of the azide group, highlighting the mildness of Ph_3PCl_2 as a chlorinating agent. Because allylic chlorides have been found to be unstable,[33,36] intermediates **17**−**19** were immediately converted to pyrophosphates **3**−**5** by reaction with tris(tetra-*n*-butylammonium) hydrogen pyrophosphate.[66,67] Following purification by ion-exchange chromatography and reverse-phase HPLC, pyrophosphates **3**−**5** were obtained in moderate yields (40−60%) from alcohols **14**−**16**, respectively.

Synthesis of Photoprobes 6 and 7. The preparation of the second class of FPP photoprobes **6** and **7** in which a flexible methylene linker chain replaces the β-isoprene of FPP is outlined in Scheme 2. Analogue **6** was designed to maximize structural overlap with FPP by replacing the terminal isoprene with *N*-methyl-*p*-azidotetrafluoroaniline and substitution of three methylenes for the β-isoprene.

An excess of ethylene glycol was monoalkylated with *p*-methoxybenzyl chloride and KOH to provide ether **20** in 66% yield after distillation. Alcohol **20** was transformed into its mesylate **21** with methanesulfonyl chloride and pyridine followed by conversion to iodide **22** in high yield via the Finkelstein reaction. Ketone **23** was obtained in 62% yield after distillation by reacting iodide **22** with sodium ethylacetoacetate followed by saponification of the resulting ester and subsequent decarboxylation. Condensation of ketone **23** with sodium triethylphosphonoacetate afforded olefin **24** in 90% yield after chromatography. Integration of ^{1}H NMR spectra and analysis of NOE experiments indicated that olefin **24** was produced in a 3:1 ratio of *E*/*Z* isomers. Repeated attempts to separate the isomers of ester **24** by column chromatography failed to improve the *E*/*Z* ratio.

Reduction of ester **24** with DIBAL-H furnished allylic alcohol **25** in 95% yield. Alcohol **25** was converted into the TBDMS ether **26** with TBDMS-Cl and imidazole. Alcohol **27** was revealed in good yield by DDQ deprotection of methoxybenzyl ether **26**. In contrast to ester **24**, the *E* and *Z* isomers of **27** were easily separated by flash chromatography. To prepare photoprobe **6**, oxidation of **27** to the corresponding aldehyde followed by reductive amination was required. Swern oxidation of the pure *E* isomer of alcohol **27** gave aldehyde **28** in 70% yield after chromatography.

N-Methyl-*p*-azidotetrafluoroaniline **31** was prepared in 81% overall yield by lithium bis(trimethylsilyl) amide deprotonation of carbamate **29**,[63] alkylation with methyl iodide to form the methyl carbamate **30**, followed by removal of the *N*-BOC group with HCl in acetic acid (Scheme 3). Reaction of equimolar amounts of aniline **31** and aldehyde **28** with $TiCl_4$, followed by $NaBH(OAc)_3$ reduction, afforded amine **34** in 60% yield after isolation. Alcohol **27** also provides the entrance to photoanalogue **6** using this scheme. Acylation of the *E* isomer of alcohol **27** with *p*-azidotetrafluorobenzoyl chloride [68] in pyridine gave benzoate **32** in high yield.

Alkyl and allylic TBDMS ethers have been converted directly into their corresponding bromides using Ph_3PBr_2 or CBr_4 and PPh_3, respectively.[69,70] We have previously found that allylic bromides are incompatible with the aniline functionality in these molecules. Consequently, we utilized Ph_3PCl_2 in CH_2Cl_2 to convert the allylic TBDMS ethers **32** and **34** into their corresponding chlorides in 87% yield. As expected, no degradation of the aryl azides by the Ph_3PCl_2 reagent was detected. Immediately after purification by flash chromatography, pyrophosphorylation of allylic chlorides **33** and **35** was effected with $(n\text{-}Bu_4N)_3HP_2O_7$.[66,67] Following ion-exchange chromatography

(64) Gribble, G. W.; Lord, P. D.; Skotnicki, J.; Dietz, S. E.; Eaton, J. T.; Johnson, J. L. *J. Am. Chem. Soc.* **1974**, *96*, 7812.
(65) Gribble, G. W.; Nutaitis, C. F. *Org. Prep. Proced. Int.* **1985**, *17*, 317−384.
(66) Davisson, V. J.; Woodside, A. B.; Poulter, C. D. *Methods Enzymol.* **1985**, *110*, 130−144.
(67) Davisson, V. J.; Woodside, A. B.; Neal, T. R.; Stremler, K. E.; Muehlbacher, M.; Poulter, C. D. *J. Org. Chem.* **1986**, *51*, 4768−4779.
(68) Keana, J. F. W.; Cai, S. X. *J. Org. Chem.* **1990**, *55*, 3640−3647.
(69) Aizpurua, J. M.; Cossio, F. P.; Palomo, C. *J. Org. Chem.* **1986**, *51*, 4941−4943.
(70) Mattes, H.; Benezra, C. *Tetrahedron Lett.* **1987**, *28*, 1697−1698.

Table 1. Comparison of pK_a of Aniline and Its Derivatives to Reaction Conditions and Yield[a]

aniline derivative	pK_a	Lewis acid	yield
aniline	4.6[b]	none	86%
p-nitroaniline	1.01[b]	none	64%
pentafluoroaniline	(-0.277 ± 0.014),[c] -0.3[d]	$TiCl_4$	60%
p-azidotetrafluoroaniline	-0.52[e]	$TiCl_4$	56%[f]
N-Me-*p*-azidotetrafluoroaniline	0.44[e]	$TiCl_4$	60%

[a] After isolation. [b] Reference 71. [c] Reference 72. [d] Reference 73. [e] Estimated, see Experimental Section. [f] *N*-Ethyl derivative.

and reverse-phase HPLC, the photoprobes **6** and **7** were obtained in 35% yield each from **32** and **34**, respectively.

Reductive Amination Conditions Depend on Amine Basicity. The basicity of the arylamine is key in choosing the appropriate reductive amination conditions to prepare compounds **2**−**6**. Table 1 lists the anilines used in this study along with their respective pK_a values. Aniline and *p*-nitroaniline have pK_a's greater than 1 and did not require imine preformation prior to $NaBH(OAc)_3$ reduction. These results suggest that conventional reductive amination methodology should be employed in the formation of allylic amines from α,β-unsaturated aldehydes when the reactant aniline has a p$K_a \geq 1$.

Analogues 2−6 Are Substrates for Farnesyltransferase In Vitro. HPLC and mass spectrometric analysis were employed to confirm that FPP and analogues **2**−**6** were transferred by FTase to the *N*-dansyl-GCVLS peptide substrate. The study of analogue **7** was discontinued because the ester was found to be hydrolytically unstable. Samples for mass spectrometry were obtained from 1 nmol scale transfer reactions for each of the pyrophosphate substrates. Reverse-phase HPLC analysis of the reaction mixtures indicated quantitative conversion of the parent peptide to the *N*-dansyl-GC(lipid)VLS peptides **43**−**47** from FPP **1** and analogues **2**−**5**, respectively. Analogue **5** was also completely transferred to *N*-biotin-GCVLS peptide to form *N*-biotin-GC(lipid)VLS **49**. Only a 50% conversion to alkylated peptide product **48** was achieved when analogue **6** was employed under these conditions. The new peaks in the HPLC chromatograms corresponding to the modified peptides were isolated, and lipid transfer was confirmed by high-resolution ESI mass spectrometry. These results indicate that transferable molecules based on the anilinogeranyl skeleton can be created that have additional functionality on the aromatic ring. As expected, the products of analogue transfer catalyzed by FTase to the peptide have increased hydrophobicity relative to the unmodified peptide which is reflected in longer retention times as compared to the parent peptide (Table 2).

Analogues 3 and 4 Are Transferred with Slightly Lower Efficiency than FPP. We have utilized a continuous fluorescence assay to determine the steady-state kinetic parameters for transfer of FPP and analogues **2**−**4** to the *N*-dansyl-GCVLS pentapeptide (Table 3).[74,75] FTase-catalyzed transfer of the analogue to the *N*-dansyl-GCVLS peptide results in a time-dependent increase in fluorescence of the dansyl group because of a local increase in hydrophobic environment around the chromophore. Initial reaction velocities were calculated from the time-dependent increase in fluorescence for reactions of FTase incubated with various concentrations of lipid pyrophosphates and 1.0 μM *N*-dansyl-GCVLS peptide (Figure 3).

Table 2. HPLC Retention Time Comparison of Isoprenyl Pyrophosphate and *N*-Dansyl-GC(lipid)VLS Peptide

substrate	HPLC t_R[a] (in min)	product	HPLC t_R *N*-dansyl-GC(lipid)VLS (in min)
FPP (**1**)	24.8	**43**	27.1
AGPP (**2**)	13.8	**44**	18.8
PFAGPP (**3**)	24.4	**45**	25.5
NAGPP (**4**)	22.7	**46**	22.5
ETAZAGPP (**5**)	26.7	**47**	25.0
MTAZA2PP (**6**)	19.9	**48**	21.3

[a] HPLC t_R *N*-dansyl-GCVLS = 13.4 min. Purified by analytical HPLC performed on a Waters HPLC controller and a Waters 2487 dual λ absorbance detector monitoring at 214 and 254 nm with a Western Analytical 250 × 4.6 mm, 5 μm BioBasic8 C_8 column. Compounds were eluted under the following gradient at a flow rate of 1 mL/min: 0−5 min 100% A, 5−37 min 10% A, 37−40 min 10% A, 40−45 min 100% A, 45−50 min 100% A. Solvents: A = 25 mM NH_4HCO_3; B = CH_3CN.

Table 3. Steady-State Kinetic Parameters[a]

substrate	K_m (nM)	k_{cat} (s^{-1}) × 10^{-2}	k_{cat}/K_m (M^{-1} s^{-1}) × 10^5	V_{rel}[b]
FPP (**1**)	46 ± 2	10 ± 0.3	22 ± 1	1.0
AGPP (**2**)	46 ± 3	8.5 ± 0.3	18 ± 1	0.85
PFAGPP (**3**)	110 ± 8	4.8 ± 0.2	4.5 ± 0.4	0.48
NAGPP (**4**)	82 ± 7	4.2 ± 0.2	5.1 ± 0.5	0.42

[a] Kinetic parameters for FPP, AGPP, PFAGPP, NAGPP measured as described in the legend of Figure 3. [b] V_{rel} refers to k_{cat}/K_m with respect to FPP.

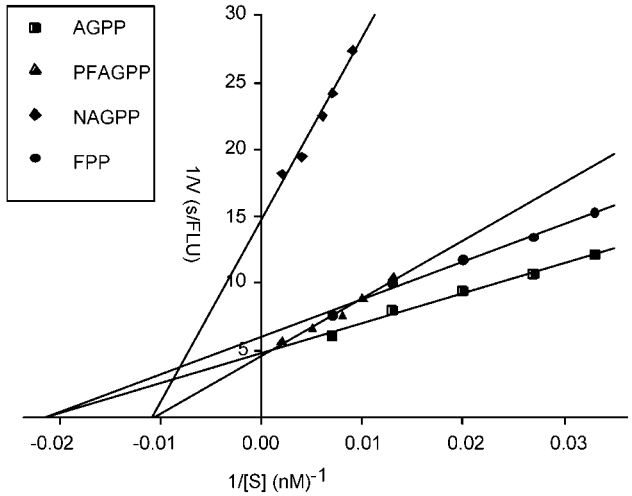

Figure 3. Lineweaver−Burke plots for FPP, AGPP, PFAGPP, and NAGPP. Each value is the average of quadruplicate incubations in the presence of the indicated concentration of FPP (■), AGPP (●), PFAGPP (▲), or NAGPP (◆), and is representative of one experiment. These assays were measured at 30 °C in 50 mM Tris·HCl, pH 7.5, 5 mM $MgCl_2$, 10 μM $ZnCl_2$, 5 mM DTT, 0.0125 mg/mL BSA, 0.04% *n*-dodecyl-β-D-maltoside with 0.15 μM FTase, 1.0 μM dansyl-GCVLS, and varying concentrations of pyrophosphate substrate distributed around the K_m (Table 3). The initial velocity was determined from the change in fluorescence. FLU represents an arbitrary fluorescence unit.

These data were used to determine the kinetic parameters K_m, k_{cat}, and k_{cat}/K_m of FPP and analogues **2**−**4** (Table 3).[37] As expected, AGPP (**2**) was found to transfer with near the same value of (k_{cat}/K_m) as FPP.[36] The analogues **3** and **4** are only slightly poorer substrates than FPP and are transferred with

(71) Dean, J. A. *Lange's Handbook of Chemistry*, 14th ed.; McGraw-Hill: New York, 1992; pp 8.19−8.71.
(72) Chiang, Y.; Grant, A. S.; Kresge, A. J.; Paine, S. W. *J. Am. Chem. Soc.* **1996**, *118*, 4366−4372.
(73) Shoute, L. C. T.; Mittal, J. P.; Neta, P. *J. Phys. Chem.* **1996**, *100*, 11355−11359.
(74) Pompliano, D. L.; Gomez, R. P.; Anthony, N. J. *J. Am. Chem. Soc.* **1992**, *114*, 7945−7946.
(75) Cassidy, P. B.; Dolence, J. M.; Poulter, C. D. *Methods Enzymol.* **1995**, *250*, 30−43.

nearly identical kinetic parameters despite structurally different ω-termini. There is no simple relationship between hydophobicity and either the K_m or the k_{cat} for analogues **2**−**4**. However, it is interesting to note that while analogue **2** and FPP share nearly identical k_{cat} and K_m, their hydrophobicities are quite different. Although analogues **5** and **6** are transferred to substrate, no increase in fluorescence was detected during the assay. This observation is not unexpected, as previous studies have shown that the fluorescence enhancement is highly dependent on the structure of the transferred lipid.[45]

Ring Fluorination and Para Substituents Have Little Effect on the Transfer Efficiency of the Analogue Pyrophosphates as Compared with FPP. For mammalian FTase, substrate binding and product release are rate-limiting for steady-state catalysis under conditions of subsaturating and saturating substrate concentrations, respectively.[76,77] The K_m for FPP does not simply reflect K_D for FPP when peptide concentration is saturating, assuming that FTase follows an ordered binding scheme.[78] The K_m for FPP may reflect the binding of FPP to the E·product complex to accelerate product dissociation.[77] Perfluorination of the aniline ring in **2** to give the isosteric PFAGPP (**3**) has only a small effect on the reaction K_m and k_{cat}, lowering the kinetic efficiency (k_{cat}/K_m) of transfer relative to analogue **2** by a factor of 5. The higher K_m and the smaller k_{cat} of pyrophosphate **3** relative to **2** suggest that formation of the FTase·**3** complex is less favored and that the dissociation rate constant of the enzyme−product complex is decreased (Table 3). Although fluorocarbons are known to interact unfavorably with both hydrocarbons and polar solvents,[79] it appears that fluorination does not significantly adversely affect the intimate contacts between the ω-terminus of the lipid and the FTase amino acid side chains in the binding site. NAGPP **4** is also accommodated by the FTase binding site in a productive fashion despite conversion of the aniline from electron donating to electron withdrawing and the increased length relative to AGPP **2**.

The quantitative FTase-catalyzed transfer of ETAZAGPP **5** to *N*-dansyl-GCVLS peptide indicates that fluorine substitution, *N*-ethylation, and the addition of a para substituent allow the analogue to bind to the enzyme in a productive fashion. Interestingly, both ETAZAGPP **5** and MTAZA2PP **6** contain a *p*-azidotetrafluoroanilino moiety in place of the FPP ω-isoprene, but these analogues are transferred to the peptide substrate with very different efficiencies. The 50% conversion of parent peptide to MTAZA2PP **6** modified product is in sharp contrast to the complete conversion that was observed for the benzyloxy substituted variable length methylene chain series of analogues **38**−**42** under similar conditions.[37] This implies that the flexible linker chain and the electronic properties of the fluorinated aniline ring compromise the kinetic efficiency of the reaction.

Modeling Indicates that the β-Isoprene of FPP and Transferable Analogues 2−5 Are Essential for Efficient Transfer. We have examined the potential FTase·analogue binding geometry of pyrophosphates **2**−**6** by docking them into the active site of the FTase crystal structure using computer modeling as previously described.[37] The procedure used to model FPP into the FTase active site reproduced the conformation and geometry of the lipid found in the X-ray crystal structures of the binary complexes.[54,56] In these complexes, electrostatic interactions between the pyrophosphate of FPP and FTase residues Lys 164β, His 248β, Arg 291β, Lys 294β, and Tyr 300β are calculated to be the dominant source of binding energy, fixing the position of the pyrophosphate with respect to the catalytic zinc ion. These electrostatic interactions were also found to be the dominant source of binding energy for the FTase models with analogues **2**−**6**. In all of the models, the pyrophosphate atoms of the analogues were found in essentially the same location as those for FPP **1** in the X-ray crystal structures. Examination of the X-ray crystal structures of the two binary FTase·FPP complexes shows that the terminal isoprene methyl groups of FPP fill a slot defined by side chains from Trp 102β, Tyr 205β, Phe 253β, Cys 254β, Trp 303β and the aliphatic stretch of Arg 202β at the bottom of the active site (Figure 4).[54,56] Between the slot and the pyrophosphate binding site, the FPP chain is fully extended and bound against the side of the active site opposite that where the incoming peptide or protein C-terminus binds. The location and conformation of the α- and β-isoprene units of analogues **2**−**6** in these models are coincident with those of the farnesyl chain in the binary complex. Except for analogue **6**, models of the complexes with analogues **2**−**5** have the terminal edge or the para substituents of the aniline group occupying the slot at the floor of the FTase active site (Figure 4). Although analogue **6** appears to be too short for the azidoaniline group to occupy the slot when its pyrophosphate is in register with the zinc ion, solvent access to the slot is blocked in the complex. The loss of these van der Waals interactions and the subsequent void in the complex may contribute to the lower efficiency of FTase-catalyzed transfer of **6** to substrate.

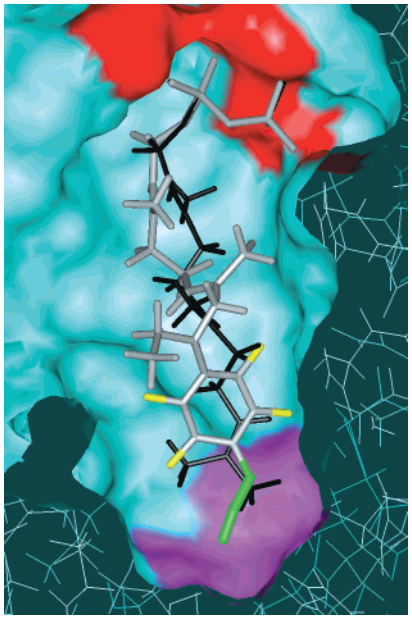

Figure 4. Cross section of FTase active site surface with pyrophosphate coordinating region in red, terminal isoprene "slot" in magenta, stick rendering of FPP in black, and of ETAZAGPP **5** in white. Note how the azide group of **5** (green) occupies the slot and how the aryl group superimposes with the terminal isoprene of FPP. Fluorines are colored yellow.

(76) Furfine, E. S.; Leban, J. J.; Landavazo, A.; Moomaw, J. F.; Casey, P. J. *Biochemistry* **1995**, *34*, 6857−6862.
(77) Tschantz, W. R.; Furfine, E. S.; Casey, P. J. *J. Biol. Chem.* **1997**, *272*, 9989−9993.
(78) Saderholm, M. J.; Hightower, K. E.; Fierke, C. A. *Biochemistry* **2000**, *40*, 12398−12405.
(79) Dunitz, J. D.; Taylor, R. *Chem.-Eur. J.* **1997**, *3*, 89−98.

In each model of the analogue complexes, the face of the aniline ring makes contact with numerous residues of the β-chain of FTase. The aromatic ring is found in the volume occupied by the terminal isoprene of FPP in the FTase·FPP complex. Interestingly, there are no qualitative differences between the aniline ring−FTase contacts in AGPP **2** and the perfluoro analogue **3**. The perfluoro aromatic ring of ETAZAGPP **5** made intimate contacts with side chains of FTase, but the *N*-ethyl group protruded into the pocket in the low energy models (Figure 4). There were no apparent specific hydrogen bonds formed between the aniline ring nitrogen of analogues **2**−**6** and the various functional groups in the pocket.

Utilizing the fluorescence transfer assay, we found that FTase does not transfer the 20-carbon GGPP **36** to protein substrate even though the longer isoprenoid is a competitive inhibitor of the enzyme.[37,80] However, previous studies with radiolabeled GGPP have shown that detectable amounts of lipid can be transferred to peptide substrate by FTase, albeit with very low efficiency.[80] Interestingly, NAGPP **4** and ETAZAGPP **5** are transferred by FTase with high efficiency despite being one to two atoms longer than FPP. In a previous study, we prepared a series of flexible FPP analogues of varying length to examine the origins of FTase discrimination for FPP **1** over the longer GGPP **36**.[37] The flexible analogues **38**−**42** were constructed by replacing the β-isoprene of FPP with a variable length methylene chain and substituting a benzyloxy group for the terminal isoprene (Figure 2). These analogues lacked the β and γ double bonds and branched methyl groups of the isoprenoids and ranged in length from the 10-carbon GPP **37** to one atom shorter than GGPP **36** in their fully extended conformations. All of these flexible analogues were transferred by FTase to substrates, but with significantly reduced rates relative to FPP **1**.

FPP **1**, AGPP **2**, PFAGPP **3**, and the flexible analogue B3PP **39** all have the same length in their extended conformations. However, B3PP **39** is transferred to substrate only 3% as efficiently as FPP, while **1**−**3** are transferred with similar efficiency (Table 2).[37] Both NAGPP **4** and ETAZAGPP **5** retain the conformationally restricted β-isoprene unit, and NAGPP **4** is transferred with twice the efficiency of the longer flexible analogues B4PP **40** and B5PP **41**.

Previously, the structural features that allowed the flexible BnPP analogues **38**−**42** to be transferred while preventing transfer of GGPP **36** were examined by modeling FPP **1**, GGPP **36**, and the flexible analogues into the active site of the FTase crystal structure.[37] The modeling indicated that within the confines of the FTase pocket, the double bonds and branched methyl groups of the geranylgeranyl chain significantly restrict the number of possible conformations relative to the more flexible lipid chain of the analogues. These conformational restrictions prevent transfer of the GGPP by forcing it to partially occlude the space occupied by the Ca_1a_2X peptide. It was further concluded that the reduced efficiency of transfer for the flexible analogues was likely due to the larger number of conformations available to them as compared with the more rigid FPP isoprene and that the lack of branched methyl groups may result in suboptimal interactions in the ternary complex. The observation that analogues **2**−**5** are transferred with a significantly higher efficiency than the flexible analogues of the same extended length reinforces the suggestion that the conformational restrictions imposed on the lipid by the β-isoprene may act to preorganize the lipid in the pocket for transfer. X-ray structural analysis has demonstrated that the peptide in the ternary complex is found in intimate contact with the farnesyl lipid.[55,56] Additional stabilization of the ternary complex for productive transfer could result from van der Waals contacts between the a_2 and X residues of the peptide and the β-isoprene unit that may be absent in the flexible analogues.

(80) Reiss, Y.; Brown, M. S.; Goldstein, J. L. *J. Biol. Chem.* **1992**, *267*, 6403−6408.

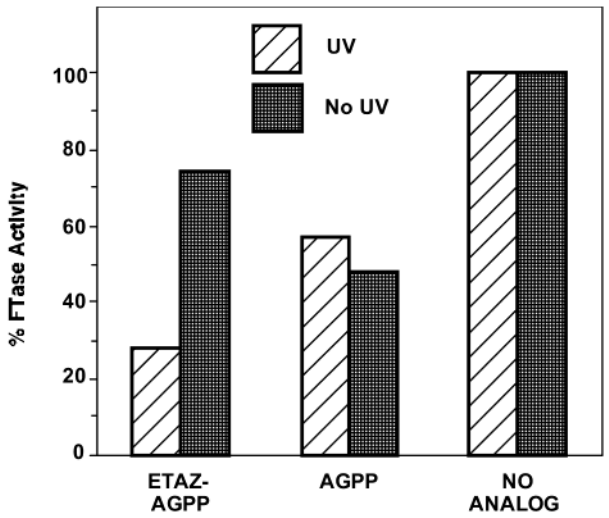

Figure 5. Photoinactivation of FTase with ETAZAGPP (**5**). FTase (10 ng) was photolyzed in the presence of 1.0 μM ETAZAGPP or 1.0 μM AGPP with 366 nm light for 30 min at 0 °C. The UV light was removed, and the samples were then incubated with 5 μM Ras and 1 μM [^{3}H]FPP (33 000 dpm/pmol) at 37 °C for 30 min in a final volume of 25 μL. The amount of [^{3}H]-prenyl transferred to Ras was determined. The 100% of [^{3}H]farnesyl transferred was 1.1 pmol. Each value is the average of duplicate experiments.

Transferable Azide Photoprobe 5 Photoinactivates FTase. Photoprobe **5** was evaluated for its ability to inactivate FTase upon UV irradiation with 366 nm light for 30 min at 0 °C. The resulting samples were assayed for residual activity by monitoring [^{3}H]-farnesyl transfer from [^{3}H]-FPP (Figure 5) to Ras. As expected, decreased FTase activity was observed when either analogue **2** or analogue **5** was incubated with Ras in the presence of FTase without UV exposure because both are alternative substrates for the enzyme. Transfer activity was further reduced by exposure of analogue **5** and FTase to longwave UV light. Irradiation of FTase at a saturating concentration of **5** (1 μM) led to a 70% overall decrease in enzyme activity. No decrease in enzyme activity was observed when FTase was irradiated with 366 nm light for 30 min in the absence of lipid analogue. These experiments indicate that FPP analogue **5** is a true photoaffinity labeling reagent because **5** inhibited FTase in a light-dependent manner.

Experimental Procedures

General Procedures. *Caution! Organic azides should be considered explosive, and all manipulations should take place behind a blast shield! Aryl azides are light sensitive, and all reactions and flash chromatography procedures should be conducted under diminished light.* All reactions were conducted under dry argon and stirred magnetically, except as noted. Reaction temperatures refer to the external bath temperatures, except as noted. Analytical TLC was performed on precoated (0.25 mm) silica gel 60F-254 (Merck) plates and developed with 30% ethyl acetate in hexane, except where noted otherwise.

Visualization was achieved either by UV irradiation, anisaldehyde-sulfuric acid spray followed by heating, or by subjecting the plates to a 5% ethanolic phosphomolybdic acid solution followed by heating. Melting points are uncorrected. Flash chromatography was performed on Merck silica gel 60 (230−400 mesh ASTM). All chromatography solvents were purchased from VWR (EM Science-Omnisolv high purity grade) and used as received. Anhydrous acetonitrile, pyridine, and DME were purchased from Aldrich, and anhydrous THF was purchased from Fluka; all other reagents were purchased either from Aldrich or from Pfaltz and Bauer, unless otherwise noted. NMR spectra were obtained in $CDCl_3$ (unless otherwise noted) at 200 or at 400 MHz. Chemical shifts for the following deuterated solvents are reported in ppm downfield using the indicated reference peaks: $CDCl_3$ ($CDCl_3$ internal peak, 7.27 ppm for ^1H, 77.4 ppm for ^{13}C), D_2O (TSP, 0 ppm ^1H and ^{13}C; H_3PO_4 as an external reference, 0 ppm for ^{31}P). Hexafluorobenzene (C_6F_6) was used as an internal reference (−162.9 ppm, 19F). Electron impact, FAB, and MALDI mass spectra were performed at the University of Kentucky Mass Spectra Facility. Combustion analyses were performed by Atlantic Microlabs, Inc., Norcross, GA. HPLC pyrophosphate purifications were monitored at 254 nm. HPLC analysis of fluorescence product studies was carried out using a Hewlett-Packard Series 1100 system equipped with a UV (monitoring at 254 nm) and fluorescence detector (340 nm excitation, 505 nm emission).

8-(*p*-Nitroaniline)-3,7-dimethyl-1-acetoxyl-2,6-octadiene (10). Into a 250 mL three-neck flask was introduced 150 mL of 1,2-dichloroethane, followed by 7.88 g (37.48 mmol) of **8**, 5.69 g (41.22 mmol) of *p*-nitroaniline, and 2.58 mL (44.89 mmol) of glacial acetic acid. After stirring for 1 min at room temperature, 11.12 g (52.47 mmol) of $NaBH(OAc)_3$ was added to the above solution. The solution was stirred at room temperature overnight, then quenched by pouring into a separatory funnel containing 200 mL of 5% $NaHCO_3$. The product was extracted with ether (3 × 75 mL), dried ($MgSO_4$), concentrated, and purified by flash chromatography (10% EtOAc in hexane) yielding 7.97 g (64%) of a bright lemon yellow oil. TLC: (R_f 0.36). ^1H NMR ($CDCl_3$, 400 MHz): δ 8.06 (m, 2H), 6.53 (m, 2H), 5.33 (m, 2H), 4.82 (bs, 1H), 4.57 (d, 2H, J = 6.8 Hz), 3.74 (d, 2H, J = 5.2 Hz), 2.18 (m, 2H), 2.10−2.03 (m, 5H), 1.69 (s, 3H), 1.66 (s, 3H). ^{13}C NMR ($CDCl_3$, 100.7 MHz): δ 171.36, 153.87, 141.47, 137.89, 131.09, 126.65, 126.47, 118.99, 111.34, 61.55, 51.02, 39.10, 25.90, 21.19, 16.56, 14.69. LRMS (EI) *m*/*z* (relative intensity): 332 (20%, M^+), 204 (100%). HRMS calcd for $C_{18}H_{24}N_2O_4$, 332.1736; found, 332.1751.

8-(Pentafluoroaniline)-3,7-dimethyl-1-acetoxyl-2,6-octadiene (11). Into a 100 mL round-bottom flask was introduced 30 mL of CH_2Cl_2 and 1.5 mL of pyridine. The solution was then deoxygenated by bubbling dry nitrogen through it for 15 min. After the addition of 5 mL of $TiCl_4$ (1 M solution in toluene, 5 mmol), the mixture was stirred for 10 min before the addition of 0.96 g (5.24 mmol) of pentafluoroaniline. The mixture was stirred for 5 min at room temperature, and a solution of 1.00 g (4.76 mmol) of aldehyde **8** in 2 mL of CH_2Cl_2 was then added in one portion to the reaction mixture. The reaction was stirred for 8 h at room temperature (TLC: R_f 0.54, imine) after which time 3 mL of glacial acetic acid was added. Stirring was continued for an additional 10 min at room temperature before the addition of 3.03 g (14.3 mmol) of $NaBH(OAc)_3$. After the reaction mixture was stirred at room temperature overnight, it was quenched with 50 mL of saturated NH_4Cl and stirred for 30 min. The mixture was then poured into 300 mL of Et_2O and washed (100 mL of water, 5% $NaHCO_3$, water, and brine). The organics were dried ($MgSO_4$), filtered, concentrated, and purified by flash chromatography (5% EtOAc in hexane) affording 1.08 g (60%) of a bright lemon yellow oil. TLC: (R_f 0.56). ^1H NMR (400 MHz): δ 5.32 (m, 2H), 4.58 (d, 2H, J = 7.1 Hz), 3.79 (s, 2H), 3.71 (bs, 1H), 2.14 (q, 2H, J = 7.9 Hz), 2.06 (s, 3H), 2.04 (t, 2H, J = 7.0 Hz), 1.69 (s, 3H), 1.65 (s, 3H). ^{13}C NMR (100.7 MHz): δ 171.52, 141.88, 139.69 (m), 137.22 (m), 135.18 (m), 132.89, 132.75 (m), 127.40, 127.36 (m), 124.07 (m), 119.08, 119.02 (m), 61.68, 54.29 (m), 39.37, 26.20, 21.40, 16.77, 14.68. ^{19}F NMR (376.7 MHz): δ −159.98 (m, 2F), −165.65 (m, 2F), −172.56 (tt, 1F, J = 6.1 Hz). LRMS (EI) *m*/*z* (relative intensity): 377 (5%, M^+), 317 (10%, M^+ − AcOH), 249 (100%). HRMS calcd for $C_{18}H_{20}F_5NO_2$, 377.1409; found, 377.1388.

8-(*p*-Azido-*N*-ethyl-tetrafluoroaniline)-3,7-dimethyl-1-acetoxyl-2,6-octadiene (12). Into a 100 mL round-bottom flask was introduced 30 mL of CH_2Cl_2 and 1.5 mL of pyridine. The solution was then deoxygenated by bubbling dry nitrogen through it for 15 min. After the addition of 5 mL of $TiCl_4$ (1 M solution in toluene, 5 mmol), the mixture was stirred for 10 min before the addition of 1.08 g (5.24 mmol) of *p*-azidotetrafluoroaniline.[63] The mixture was stirred for 5 min at room temperature, and a solution of 1.00 g (4.76 mmol) of aldehyde **8** in 2 mL of CH_2Cl_2 was then added in one portion to the reaction mixture. The reaction was stirred for 8 h at room temperature (TLC: R_f 0.54, imine) after which time 3 mL of glacial acetic acid was added. Stirring was continued for an additional 10 min at room temperature before the addition of 3.03 g (14.3 mmol) of $NaBH(OAc)_3$. After the mixture was stirred at room temperature for 24 h, an additional 3.03 g (14.3 mmol) of $NaBH(OAc)_3$ and 1 mL of glacial acetic acid was added, and the mixture was stirred for another 24 h at room temperature. The reaction mixture was then quenched with 10 mL of water and stirred for 30 min. The mixture was poured into 300 mL of Et_2O and washed (100 mL of water, 5% $NaHCO_3$, water, and brine). The organics were then dried ($MgSO_4$), filtered, and concentrated to give a blood-red oil. Purification by flash chromatography (5% EtOAc in hexane) yielded 1.15 g (56%) of a pale-yellow oil that rapidly turned pale-orange. TLC: (R_f 0.62). ^1H NMR (400 MHz): δ 5.32 (m, 2H), 4.57 (d, 2H, J = 6.8 Hz), 3.61 (s, 2H), 3.09 (q, 2H, J = 7.2 Hz), 2.33 (m, 2H), 2.05 (s, 3H), 2.04 (m, 2H), 1.69 (s, 3H), 1.59 (s, 3H), 1.01 (t, 3H, J = 7.2 Hz). ^{13}C NMR (100.7 MHz): δ 171.33, 146.24 (m), 143.79 (m), 142.45 (m), 141.93, 140.06 (m), 132.69, 127.88, 125.88 (m), 118.73 (s + m), 61.51, 61.23 (m), 46.95 (m), 39.28, 26.06, 21.22, 16.56, 14.32, 13.01. ^{19}F NMR (376.7 MHz): δ −148.66 (m, 2F), −154.32 (m, 2F). IR (KBr): 2122, 1740, 1492. LRMS (EI) *m*/*z* (relative intensity): 428 (45%, M^+), 402 (100%, $M^+ - N_2 + 2H$), 249 (70%). HRMS calcd for $C_{20}H_{24}F_4N_4O_2$, 428.1830; found, 428.1821.

General Saponification Conditions for Compounds 14−16. To a 100 mL round-bottom flask were added the acetate (5.56 mmol) and 50 mL of methanol. Potassium carbonate (2.31 g, 16.7 mmol) dissolved in 10 mL of water was added, and the reaction mixture was stirred at room temperature overnight. Water was added (20 mL), and the mixture was extracted with CH_2Cl_2 (3 × 100 mL). The combined extracts were washed once with brine (100 mL), dried ($MgSO_4$), and concentrated.

8-(*p*-Nitroaniline)-3,7-dimethyl-2,6-octadien-1-ol (14). 1.50 g (93%) of a bright lemon yellow oil. TLC: (R_f 0.10). ^1H NMR ($CDCl_3$, 400 MHz): δ 8.07 (m, 2H), 6.53 (m, 2H), 5.38 (m, 2H), 4.90 (bs, 1H), 4.15 (d, 2H, J = 6.4 Hz), 3.73 (s, 2H), 2.18 (m, 2H), 2.05 (t, 2H, J = 7.6 Hz), 1.66 (bs, 6H). ^{13}C NMR ($CDCl_3$, 100.7 MHz): δ 153.88, 138.99, 137.92, 131.06, 126.97, 126.52, 123.99, 111.34, 59.47, 51.12, 39.15, 25.98, 16.37, 14.78. LRMS (EI) *m*/*z* (relative intensity): 290 (70%, M^+), 204 (100%). HRMS calcd for $C_{16}H_{22}N_2O_3$, 290.1630; found, 290.1640.

8-(Pentafluoroaniline)-3,7-dimethyl-2,6-octadien-1-ol (15). 1.78 g (96%) of a pale-yellow oil. TLC: (R_f 0.20). ^1H NMR (400 MHz): δ 5.37 (m, 2H), 4.15 (d, 2H, J = 7.0 Hz), 3.79 (s, 2H), 2.31 (bs, 2H), 2.14 (q, 2H, J = 7.0 Hz), 2.03 (t, 2H, J = 7.2 Hz), 1.67 (s, 3H), 1.65 (s, 3H). ^{13}C NMR (100.7 MHz): δ 139.71 (m), 139.47, 137.30 (m), 135.23 (m), 132.77 (s + m), 127.61 (s + m), 124.08 (s + m), 59.70, 54.33 (m), 39.39, 26.29, 16.58, 14.70. ^{19}F NMR (376.7 MHz): δ −159.82 (d, 2F, J = 22 Hz), −165.61 (m, 2F), −172.37 (m, 1F). LRMS (EI) *m*/*z* (relative intensity): 335 (15%, M^+), 249 (85%), 196 (100%). HRMS calcd for $C_{16}H_{18}F_5NO$, 335.1303; found, 335.1311.

8-(*p*-Azido-*N*-ethyl-tetrafluoroaniline)-3,7-dimethyl-2,6-octadien-1-ol (16). 2.08 g (97%) of a viscous, orange colored oil. TLC: (R_f 0.20). ^1H NMR (400 MHz): δ 5.35 (m, 2H), 4.14 (d, 2H, J = 6.8 Hz), 3.61 (s, 2H), 3.09 (q, 2H, J = 7.2 Hz), 2.13 (m, 4H), 1.66 (s, 3H), 1.60 (s, 3H), 1.34 (bs, 1H), 1.01 (t, 3H, J = 7.2 Hz). ^{13}C NMR (100.7

MHz): δ 146.17 (m), 143.72 (m), 142.44 (m), 139.97 (m), 139.39, 132.57, 128.03, 125.86 (m), 123.79, 114.13 (m), 61.24 (m), 59.51, 46.98 (m), 39.30, 26.15, 16.35, 14.30, 13.02. ^{19}F NMR (376.7 MHz): δ −149.35 (m, 2F), −155.05 (m, 2F). IR (KBr): 2122, 1492. LRMS (EI) *m*/*z* (relative intensity): 386 (15%, M^+), 358 ($M^+ - N_2$, 5%), 135 (60%), 93 (100%). HRMS calcd for $C_{18}H_{22}F_4N_4O$, 386.1730; found, 386.1737.

General Halogenation Conditions for Compounds 17−19. Into a 100 mL round-bottom flask were added the allylic alcohol (5.05 mmol), *N*,*N*-diisopropylethylamine (1.41 mL, 8.09 mmol), and 30 mL of dry acetonitrile. The solution was stirred at 0 °C for 10 min. Solid dichlorotriphenylphosphorane (2.45 g, 7.58 mmol) was then added evenly to the reaction mixture over a 7 min period. After the final addition of Ph_3PCl_2, the reaction was allowed to stir at 0 °C for an additional 40 min. The mixture was then loaded directly onto a silica gel column and purified by flash chromatography (5% EtOAc in hexane).

8-(*p*-Nitroaniline)-3,7-dimethyl-1-chloro-2,6-octadiene (17). 1.17 g (75%) of a bright lemon yellow oil. TLC: (R_f 0.56).

8-(Pentafluoroaniline)-3,7-dimethyl-1-chloro-2,6-octadiene (18). 1.48 g (83%) of a yellow oil. TLC: (R_f 0.56).

8-(*p*-Azido-*N*-ethyl-tetrafluoroaniline)-3,7-dimethyl-1-chloro-2,6-octadiene (19). 1.74 g (85%) of a pale-yellow oil which rapidly turned orange. TLC: (R_f 0.68).

General Pyrophosphorylation Conditions for Compounds 3−5. Into a 50 mL glass centrifuge tube was added 7.45 g (7.6 mmol) of tris(tetrabutylammonium) hydrogen pyrophosphate and 12 mL of dry acetonitrile. After vortexing, the milky white solution was then centrifuged at 2000 rpm for 10 min. The clear supernatant was decanted into a flame-dried, 100 mL, round-bottomed flask charged with the allylic chloride (3.8 mmol). The solution was allowed to stir at room temperature for 4 h. Solvent was removed, and the residue was dissolved in 3 mL of ion-exchange buffer (ion-exchange buffer was generated by dissolving ammonium bicarbonate (2.0 g, 25.3 mmol) in 1.0 L of 2% (v/v) isopropyl alcohol/water). The resulting milky solution was loaded onto a preequilibrated 2 × 30 cm column of Dowex AG 50W-X8 (100−200 mesh) cation-exchange resin (NH_4^+ form). The flask was washed twice with 5 mL of buffer, and both washes were loaded onto the column before elution with 190 mL (two column volumes) of ion-exchange buffer. The cloudy eluant was collected in a 600 mL freeze-drying flask, frozen, and lyophilized. A portion of the crude pyrophosphate was dissolved in 25 mM NH_4HCO_3 to a final concentration of ca. 5 mM. The solution was loaded onto a preparative Western Analytical 250 × 10 mm, 5 μm BioBasic8 C_8 column and eluted under the following gradient at a flow rate of 4 mL/min: 0−11 min 100% A, 11−12 min 80% A, 12−24 min 80% A, 24−27 min 5% A, 27−31 min 5% A, 31−36 min 100% A, 36−45 min 100% A. Solvents, A = 25 mM NH_4HCO_3; B = 2-propanol:acetonitrile (1:1 v/v). The desired peak was collected, frozen, and lyophilized.

8-(*p*-Nitroaniline)-3,7-dimethyl-2,6-octadiene Pyrophosphate (3). Bright lemon yellow solid (54%). ^{1}H NMR (D_2O, 400 MHz): δ 8.09 (m, 2H), 6.69 (m, 2H), 5.42 (m, 2H), 4.46 (t, 2H, J = 7.0 Hz), 3.81 (s, 2H), 2.21 (q, 2H, J = 6.8 Hz), 2.10 (t, 2H, J = 7.3 Hz), 1.70 (s, 3H), 1.65 (s, 3H). ^{13}C NMR (D_2O, 100.7 MHz): δ 158.26, 145.37, 138.84, 134.51, 129.85, 128.75, 122.88 (d, J = 9.2 Hz), 114.50, 65.55 (d, J = 5.3 Hz), 52.45, 41.35, 28.12, 18.47, 16.46. ^{31}P NMR (D_2O, 162.1 MHz): δ −7.65 (d, 1P, J = 22 Hz), −9.62 (d, 1P, J = 21 Hz). LRMS (FAB$^-$, glycerol matrix): calculated $(M - H)^-$, 449.1; measured, 449.1.

8-(Pentafluoroaniline)-3,7-dimethyl-2,6-octadiene Pyrophosphate (4). White solid (60%). ^{1}H NMR (D_2O, 400 MHz): δ 5.37 (dt, 2H, J = 7.0 Hz), 4.46 (t, 2H, J = 6.6 Hz), 3.72 (s, 2H), 2.11 (q, 2H, J = 7.3 Hz), 1.99 (t, 2H, J = 7.1 Hz), 1.67 (s, 3H), 1.62 (s, 3H). ^{13}C NMR (D_2O, 100.7 MHz): δ 145.66, 143.65 (m), 141.90 (m), 141.23 (m), 139.45 (m), 135.39, 130.99, 125.27 (m), 122.36 (d, J = 7.7 Hz), 65.68 (d, J = 5.3 Hz), 56.64 (m), 41.29, 28.24, 18.40, 16.10. ^{19}F NMR (D_2O, 376.7 MHz): δ −155.86 (d, 2F, J = 21 Hz), −164.73 (t, 2F, J = 21 Hz), −168.47 (t, 1F, J = 22 Hz). ^{31}P NMR (D_2O, 162.1 MHz): δ −9.16 (m, 1P, J = 22 Hz), −9.71 (m, 1P, J = 21 Hz). LRMS (FAB$^-$, glycerol matrix): calculated $(M - H)^-$, 494.1; measured, 494.1.

8-(*p*-Azido-*N*-ethyl-tetrafluoroaniline)-3,7-dimethyl-2,6-octadiene Pyrophosphate (5). White solid (57%). ^{1}H NMR (D_2O, 400 MHz): δ 5.40 (t, 1H, J = 7.0 Hz), 5.35 (t, 1H, J = 6.2 Hz), 4.47 (t, 2H, J = 6.2 Hz), 3.62 (s, 2H), 3.11 (q, 2H, J = 7.3 Hz), 2.08 (q, 2H, J = 6.8 Hz), 1.94 (t, 2H, J = 7.3 Hz), 1.67 (s, 3H), 1.60 (s, 3H), 0.99 (t, 3H, J = 7.1 Hz). ^{13}C NMR (D_2O, 100.7 MHz): δ 149.77 (m), 147.42 (m), 145.53, 144.95 (m), 142.51 (m), 134.66, 132.77 (m), 125.67 (m), 122.36 (m), 119.27 (m), 65.64 (d, J = 5.3 Hz), 65.10 (m), 51.42 (m), 41.20, 28.21, 18.41, 17.01, 14.72. ^{19}F NMR (D_2O, 376.7 MHz): δ −147.07 (m, 2F), −153.99 (m, 2F). ^{31}P NMR (D_2O, 162.1 MHz): δ −8.76 (m, 1P, J = 20 Hz), −9.75 (m, 1P, J = 21 Hz). LRMS (FAB$^-$, glycerol matrix): calculated $(M - H)^-$, 545.1; measured, 545.1. HRMS (ESI): calculated $(M + H)^+$ $C_{18}H_{25}F_4N_4O_7P_2$, 547.1135; measured, 547.1124.

(*p*-Methoxybenzyloxy)ethanol (20). Solid potassium hydroxide (86%, 2.4 g, 3.8 mmol) was added to ethylene glycol (21 mL, 38 mmol) and stirred until dissolution. The temperature was then increased to 130 °C (internal temperature) and maintained at this temperature until the water stopped collecting in the air condenser (ca. 2−3 h). The reaction was cooled to room temperature, and *p*-methoxybenzyloxy chloride (6 g, 3.8 mmol) was added. The temperature was then raised to 35 °C and kept at this point overnight. The reaction mixture was then cooled, diluted with water (80 mL), and extracted with Et_2O. The extract was washed with water, dried ($MgSO_4$), filtered, and evaporated. The residue was purified by distillation under reduced pressure to afford 4.6 g (66%) of **20** as a colorless oil: bp 132 °C/0.35 mmHg (lit.[71] 145−146 °C/5 mmHg). ^{1}H NMR (200 MHz): δ 7.32−7.20 (m, 2H), 6.94−6.80 (m, 2H), 4.48 (s, 2H), 3.79 (s, 3H), 3.75−3.70 (m, 2H), 3.58−3.53 (m, 2H), 2.26 (bs, 1H). ^{13}C NMR (50 MHz): δ 159.65, 130.41, 129.77, 114.19, 73.26, 71.44, 62.18, 55.59.

(*p*-Methoxybenzyloxy)ethyl Methanesulfonate (21). To a cooled (0 °C) solution of the alcohol **20** (14.8 g, 81 mmol) in anhydrous pyridine (34 mL) was added methanesulfonyl chloride (9.4 mL, 121.5 mmol). The reaction mixture was warmed to room temperature, stirred for 2 h, and then diluted with water and extracted with Et_2O. The organic solution was washed (10% HCl, then water, then 10% $NaHCO_3$, then water), dried ($MgSO_4$), filtered, and evaporated to obtain 16.85 g (80%) of a colorless oil that was used in the next step without further purification. The analytical sample was obtained by flash chromatography (20% EtOAc in hexane) to give **21** as a colorless oil. ^{1}H NMR (400 MHz): δ 7.32−7.21 (m, 2H), 6.94−6.84 (m, 2H), 4.51 (s, 2H), 4.41−4.36 (m, 2H), 3.81 (s, 3H), 3.73−3.69 (m, 2H), 3.03 (s, 3H). ^{13}C NMR (100 MHz): δ 159.77, 129.83, 129.77, 114.24, 73.35, 69.57, 67.82, 55.64, 38.05. LRMS (EI) *m*/*z* (relative intensity): 260 (65%, M^+), 121 (100%). HRMS calcd for $C_{11}H_{16}O_5S$, 260.0699; found, 260.0699. Anal. Calcd for $C_{11}H_{16}O_5S$: C, 50.76; H, 6.19; S, 12.32. Found: C, 50.60; H, 6.05; S, 12.10.

(*p*-Methoxybenzyloxy)ethyl Iodide (22). To a solution of NaI (32 g, 213 mmol) in acetone (140 mL) was added at room temperature a solution of the methanesulfonate **21** (18.4 g, 71 mmol) in acetone (30 mL). After the mixture was stirred at room temperature overnight, water was added, and the product was extracted with Et_2O. The organic phase was washed (10% $Na_2S_2O_3$, then water), dried ($MgSO_4$), filtered, and evaporated to obtain 18.66 g (90%) of the desired iodide as a slightly yellow oil that was used without further purification. The analytical sample was purified by flash chromatography (10% EtOAc in hexane) to give iodide **22** as a colorless oil. ^{1}H NMR (200 MHz): δ 7.31−7.25 (m, 2H), 6.91−6.86 (m, 2H), 4.51 (s, 2H), 3.81 (s, 3H), 3.71 (t, 2H, J = 6.8 Hz), 3.26 (t, 2H, J = 6.8 Hz). ^{13}C NMR (50 MHz): δ 159.81, 130.27, 129.76, 114.26, 72.84, 70.81, 55.58, 3.28. LRMS (EI) *m*/*z* (relative intensity): 292 (52%, M^+), 121 (100%). HRMS calcd for $C_{10}H_{13}O_2I$, 291.9955; found, 291.9947.

5-(*p*-Methoxybenzyloxy)-pentan-2-one (23). To a solution of ethylacetoacetate sodium salt (19.5 g, 128 mmol) in anhydrous DME

(180 mL) at room temperature was added a solution of the iodide **22** (18.7 g, 64 mmol) in anhydrous DME (15 mL), and the reaction mixture was heated at reflux overnight. After cooling to room temperature, a solution of NaOH (14.2 g, 350 mmol) in water (142 mL) was added, the mixture was refluxed for 2 h, cooled to room temperature, acidified with 50% H_2SO_4 (40 mL, final pH $\approx$ 2), and then refluxed for 2 h more. Water was added, and the product was extracted with Et_2O. The organic phase was washed (10% $NaHCO_3$ then water), dried ($MgSO_4$), filtered, and evaporated to obtain an oily residue. Purification by distillation under reduced pressure gave 8.81 g (62%) of ketone **23** as a pale-yellow oil: bp 110 °C/0.25 mmHg. ^{1}H NMR (200 MHz): δ 7.27−7.22 (m, 2H), 6.89−6.85 (m, 2H), 4.41 (s, 2H), 3.80 (s, 3H), 3.45 (t, 2H, J = 6.2 Hz), 2.53 (t, 2H, J = 7.1 Hz), 2.13 (s, 3H), 1.93−1.80 (qui, 2H). ^{13}C NMR (50 MHz): δ 209.02, 159.56, 130.90, 129.61, 114.16, 72.91, 69.37, 55.66, 40.74, 30.32, 24.29. IR (KBr): 1716, 1514, 1243. LRMS (EI) *m*/*z* (relative intensity): 222 (5%, M^+), 121 (100%). HRMS calcd for $C_{13}H_{18}O_3$, 222.1250; found, 222.1258. Anal. Calcd for $C_{13}H_{18}O_3$: C, 70.24; H, 8.16. Found: C, 70.31; H, 8.14.

Ethyl 6-(*p*-Methoxybenzyloxy-3-methyl-hex-2-enoate (24). Triethylphosphonoacetate (16.6 g, 74 mmol) was added dropwise to a stirred suspension of NaH (1.8 g, 74 mmol) in dry THF (45 mL) at 0 °C and allowed to stir for 30 min. A solution of the ketone **23** (8.3 g, 37 mmol) in dry THF (30 mL) was then added at the same temperature. After the reaction was allowed to warm to room temperature and stirred overnight, it was then diluted with saturated NH_4Cl and extracted with Et_2O. The ether layer was washed with water, dried ($MgSO_4$), filtered, and evaporated to give an oily residue. Purification by flash chromatography on silica gel (20% EtOAc in hexane) gave 9.73 g (90%) of olefin **24** as a colorless oil and as an *E*/*Z* mixture in the ratio ~75:25 which was used to the next reaction without further separation. ^{1}H NMR (400 MHz) (isomers *Z* and *E*): δ 7.27−7.24 (m, 2H), 6.88−6.86 (m, 2H), 5.67−5.66 (m, 1H), 4.43 and 4.41 (two singlets, 2H, isomers *Z* and *E*, respectively), 4.16−4.09 (m, 2H), 3.79 (s, 3H), 3.49 and 3.43 (two triplets, 2H, J = 6.6 Hz for isomer *Z* and J = 6.2 Hz for isomer *E*), 2.70−2.66 (m, 2H from isomer *Z*), 2.24−2.01 (m, 2H, from isomer *E*), 2.15 and 1.88 (two dublets, 3H, J = 1.2 Hz for isomer *E* and J = 1.2 Hz for isomer *Z*), 1.82−1.73 (m, 2H), 1.29−1.22 (m, 3H). ^{13}C NMR (100 MHz) (isomers *Z* and *E*): δ 167.11, 159.73, 159.49, 130.81, 129.56, 116.71, 116.09, 114.09, 114.04, 72.92, 72.88, 70.29, 69.42, 59.77, 55.54, 37.79, 30.47, 30.02, 28.62, 27.82, 25.52, 19.03, 14.64. IR (KBr): 1708, 1508, 1243. LRMS (EI) *m*/*z* (relative intensity): 292 (5%, M^+), 121 (100%). HRMS calcd for $C_{17}H_{24}O_4$, 292.1645; found, 292.1645.

6-(*p*-Methoxybenzyloxy)-3-methyl-hex-2-enol (25). To the solution of ester **24** (9.6 g, 33 mmol) in 150 mL of dry THF under argon at −78 °C was added diisobutyl aluminum hydride (1.5 M solution in toluene, 88 mL, 132 mmol). The reaction was stirred at −78 °C for 2 h. A 10% (w/v) solution of potassium sodium tartrate was added, and the reaction mixture was allowed to warm to room temperature. After dilution with water, the mixture was extracted with Et_2O (2×). The combined organic layers were washed (water then brine), dried over $MgSO_4$, and evaporated to obtain 7.85 g (95%) of an oily residue that was used in the next step without further purification. The analytical sample was purified by flash chromatography (30% Et_2O in hexane) giving alcohol **25** as a colorless oil. ^{1}H NMR (200 MHz) (isomer *E*): δ 7.28−7.24 (m, 2H), 6.89−6.86 (m, 2H), 5.44−5.35 (m, 1H), 4.42 (s, 2H), 4.12 (d, 2H, J = 7 Hz), 3.80 (s, 3H), 3.43 (t, 2H, J = 6.6 Hz), 2.14−2.01 (m, 2H), 1.80−1.67 (m, 2H), 1.66 (s, 3H). ^{13}C NMR (50 MHz) (isomer *E*): δ 159.42, 139.56, 130.95, 129.42, 123.81, 113.98, 72.67, 69.66, 59.49, 55.38, 36.08, 27.85, 16.22. LRMS (EI) *m*/*z* (relative intensity): 250 (3.5%, M^+), 121 (100%). Anal. Calcd for $C_{15}H_{22}O_3$: C, 71.97; H, 8.86. Found: C, 71.76; H, 8.86.

1-(*tert*-Butyldimethylsilyloxy)-6-(*p*-methoxybenzyloxy)-3-methyl-hex-2-ene (26). To a solution of allylic alcohol **25** (7.4 g, 29.6 mmol) in dry DMF was added imidazole (2.4 g, 35.5 mmol) followed by *tert*-butyldimethylsilyl chloride (5.4 g, 35.5 mmol). The reaction was stirred at room temperature overnight. The reaction mixture was then diluted with water and extracted with hexane. The combined organic layers were washed with water, dried ($MgSO_4$), filtered, and evaporated. Purification by flash chromatography (25% Et_2O in hexane) afforded 10.25 g (95%) of silyl ether **26** as a colorless oil. ^{1}H NMR (400 MHz) (isomer *E*): δ 7.28−7.24 (m, 2H), 6.89−6.86 (m, 2H), 5.33−5.29 (m, 1H), 4.42 (s, 2H), 4.18 (dd, 2H, J = 6.2 Hz, J = 0.4 Hz), 3.80 (s, 3H), 3.43 (t, 2H, J = 6.4 Hz), 2.08−2.04 (m, 2H), 1.76−1.69 (m, 2H), 1.61 (d, 3H, J = 0.8 Hz), 0.9 (s, 9H), 0.06 (s, 6H). ^{13}C NMR (100 MHz) (isomer *E*): δ 159.48, 136.83, 131.09, 129.61, 124.99, 114.13, 72.94, 70.12, 60.66, 55.64, 36.34, 28.16, 26.39, 18.79, 16.66, −4.66. LRMS (CI) *m*/*z* (relative intensity): 365 (5%, MH^+), 307 (40%, M − $C_4H_9^+$), 243 (65%, M − $C_8H_9O^+$). Anal. Calcd for $C_{21}H_{36}O_3Si$: C, 69.18; H, 9.95. Found: C, 69.23; H, 9.84.

1-(*tert*-Butyldimethylsilyloxy)-3-methyl-hex-2-en-6-ol (27). Solid DDQ (480 mg, 2.1 mmol) was added in one portion to a solution of **26** (533 mg, 1.46 mmol) in 5.5 mL of 0.1 M sodium phosphate buffer (pH 7.2) and CH_2Cl_2 (55 mL), and the resultant mixture was vigorously stirred for 2.5 h at room temperature. The mixture was then filtered through a silica gel pad, and the filter cake was washed with 1:1 (v/v) ether:hexane. The colorless filtrate was concentrated and purified by flash chromatography (5% EtOAc in hexane, then 10% EtOAc in hexane) to give 186 mg (52%) of **27** as *Z* isomer, and 62 mg (17%) of **27** as *E* isomer.

***Z*-1-(*tert*-Butyldimethylsilyloxy)-3-methyl-hex-2-en-6-ol (*Z*-27).** R_f 0.56. ^{1}H NMR (200 MHz): δ 5.50−5.40 (m, 1H), 4.15 (d, 2H, J = 7.2 Hz), 3.61−3.55 (m, 2H), 2.22 (t, 2H, J = 7 Hz), 1.73 (s, 3H), 1.72−1.50 (m, 2H), 0.91 (s, 9H), 0.09 (s, 6H).

***E*-1-(*tert*-Butyldimethylsilyloxy)-3-methyl-hex-2-en-6-ol (*E*-27).** R_f 0.52. ^{1}H NMR (200 MHz): δ 5.40−5.31 (m, 1H), 4.09 (dd, 2H, J = 6.2 Hz, J = 0.6 Hz), 3.65 (m, 2H), 2.12−2.05 (m, 2H), 1.72 (m, 2H), 1.64 (s, 3H), 1.57 (bs, 1H), 0.90 (s, 9H), 0.07 (s, 6H). ^{13}C NMR (50 MHz): δ 137.11, 125.25, 63.10, 60.55, 36.17, 30.96, 26.33, 18.72, 16.55, −4.77. LRMS (CI) *m*/*z* (relative intensity): 245 (10%, MH^+), 243 (5%, M − H^+), 229 (7%, M − CH_3^+), 187 (100%, M − $C_4H_9^+$). Anal. Calcd for $C_{13}H_{28}O_2Si$: C, 63.88; H, 11.54. Found: C, 63.73; H, 11.58.

6-(*tert*-Butyldimethylsilyloxy)-3-methyl-hex-2-enal (28). The *E* isomer of alcohol **27** (218 mg, 0.89 mmol) in 3 mL of CH_2Cl_2 was added to a premixed solution of oxalyl chloride (0.15 mL, 1.37 mmol) and DMSO (0.19 mL, 2.67 mmol) in 5 mL of CH_2Cl_2 at −78 °C. The resulting mixture was stirred for 30 min, and triethylamine (0.65 mL, 4.7 mmol) was then added. After being stirred for an additional 15 min at −78 °C, the reaction was allowed to warm to room temperature and was stirred for 30 min longer. The reaction mixture was then quenched with water and extracted with CH_2Cl_2. The combined extracts were washed (water then brine), dried ($MgSO_4$), and concentrated. Purification by flash chromatography (hexane/diethyl ether 8:1) afforded 142 mg (66%) of aldehyde **28** as a colorless oil. ^{1}H NMR (400 MHz): δ 9.78 (t, J = 1.8 Hz, 1H), 5.32 (m, 1H), 4.18 (m, 2H), 2.56 (m, 2H), 2.34 (t, 2H, J = 7.6 Hz), 1.65 (m, 3H), 0.89 (s, 9H), 0.06 (s, 6H). ^{13}C NMR (50 MHz): δ 216.52, 135.16, 125.88, 60.26, 42.29, 31.93, 26.39, 18.80, 16.86, −4.70. IR (KBr): 1728. LRMS (EI) *m*/*z* (relative intensity): 241 (2%, M − H^+), 185 (55%, M − ^{t}Bu), 75 (100%). HRMS calcd for $C_{12}H_{23}O_2Si$ (M − Me), 227.1462; found, 227.1423. $C_9H_{17}O_2Si$ (M − ^{t}Bu), 185.0907; found, 185.0992.

4-(*N*-Methyl-*N*-*tert*-butoxycarbonylamino)tetrafluorophenyl Azide (30). The carbamate **29** (1.0 mmol) was dissolved in 10 mL of anhydrous THF and cooled to −78 °C. Next 1.2 mL (1.2 mmol) of lithium bis(trimethylsilyl)amide (1 M solution in THF) was added. The solution was stirred for 30 min, and methyl iodide (0.1 mL, 1.55 mmol) was added. The reaction was warmed to 5 °C and kept at this temperature overnight. Water was then added, and the reaction was extracted with Et_2O. The combined organic extracts were washed (1 N HCl, then water), dried ($MgSO_4$), filtered, and evaporated. The residue was purified by chromatography on silica gel (hexane/diethyl ether 8:1)

to give 297 mg (93%) of **30**. ^{1}H NMR (400 MHz): δ 3.17 (s, 3H), 1.53 and 1.39 (two singlets from minor and major rotamers, respectively, 9H). ^{13}C NMR (100 MHz): δ 154 and 153.8 (minor and major rotamers, respectively), 144 (m) and 149.82 (m) (minor and major rotamers, respectively), 143 (m) and 142.83 (m) (minor and major rotamers, respectively), 142.3 (m), 139.8 (m), 125.91, 119 (m), 82.5 and 82.1 (minor and major, respectively), 37.5 and 36.5 (minor and major rotamers, respectively), 28.53 and 28.33 (minor and major rotamers, respectively). ^{19}F NMR (376 MHz): $-$146.93 (m) and $-$147.57 (m) (minor and major rotamers, respectively), $-$153.69 and $-$153.95 (m) (minor and major rotamers, respectively). IR (KBr): 2120, 1716, 1506. LRMS (EI) *m*/*z* (relative intensity): 320 (8%, M^+), 247 (30%, M $-$ ^{t}BuO), 57 (100%). HRMS calcd for $C_{12}H_{12}F_4N_4O_2$ (M^+), 320.0891; found, 320.0813. $C_8H_3F_4N_4O$ (M $-$ ^{t}BuO), 247.0238; found, 247.0209.

***N*-Methyl-4-azidotetrafluoroaniline (31).** Carbamate **30** (108 mg, 0.34 mmol) was dissolved in anhydrous CH_2Cl_2 (5 mL) at 0 °C, and 1.2 mL of 1 N HCl in AcOH (Aldrich) was added. The reaction was slowly (ca 2 h) allowed to warm to room temperature and stirred overnight. Next 4 mL of water was added, and the reaction was extracted with hexane:diethyl ether (1:1 v/v). The organic layers were washed (5% $NaHCO_3$ then water), dried ($MgSO_4$), filtered through a pad of silica gel, and concentrated to afford 70 mg (94%) of **31** which was used in the next reaction without further purification. ^{1}H NMR (500 MHz): δ 4.78 (bs, 1H), 3.08 (m, 3H). ^{13}C NMR (100 MHz): δ 142.8 (m), 140.4 (m), 139.1 (m), 136.7 (m), 126.2 (m), 107.7 (m), 33.34 (t). ^{19}F NMR (470 MHz): δ $-$154.49 (m), $-$160.85 (m). IR (KBr): 2116, 1509. LRMS (EI) *m*/*z* (relative intensity): 219 (75%, M $-$ H^+), 192 (100%, M $-$ N_2).

***N*-(6-(*tert*-Butyldimethylsilyloxy)-4-methyl-4-hexenyl)-*N*-methyl-4-azidotetrafluoroaniline (34).** A solution of pyridine (0.1 mL) in CH_2Cl_2 (5 mL) was cooled to $-$78 °C, and 0.3 mL (0.3 mmol) of $TiCl_4$ (1 M solution in toluene) was slowly added. The mixture was then stirred for 10 min followed by the dropwise addition of amine **31** (66 mg, 0.30 mmol) in dry CH_2Cl_2 (2 mL). The reaction mixture was stirred for 5 min at $-$78 °C, and then a solution of aldehyde **28** (72 mg, 0.30 mmol) in 1 mL of dry CH_2Cl_2 was added in one portion. The reaction mixture was allowed to warm to room temperature and was stirred overnight. After 0.38 mL (6.6 mmol) of glacial acetic acid was added, the mixture was stirred for 10 min, and $NaBH(OAc)_3$ (263 mg, 1.2 mmol) was added in one portion. The reaction was stirred at room temperature for 20 h, diluted with 5 mL of hexane, and poured into a separatory funnel containing 10 mL of hexane and 10 mL of a saturated solution of NH_4F. The aqueous layer was extracted with hexane, and the combined organic layers were washed (5% $NaHCO_3$, then water), dried ($MgSO_4$), filtered, and evaporated. The residue was purified by flash chromatography (4% Et_2O in hexane) affording 80 mg (60%) of compound **34**. ^{1}H NMR (400 MHz): δ 5.29$-$5.25 (m, 1H), 4.17 (dd, 2H, J = 6.4 Hz, J = 0.8 Hz), 3.08 (t, 2H, J = 7.6 Hz), 2.89 (t, J = 2 Hz), 1.99 (t, J = 7.6 Hz), 1.65$-$1.59 (m, 5H), 0.89 (s, 9H), 0.06 (s, 6H). ^{13}C NMR (100 MHz): δ 145.01 (m), 142.6 (m), 140.18 (m), 136.27, 127.5 (m), 125.1, 113 (m), 60.40, 55.28 (t, J = 3 Hz), 41.08 (t, J = 3.1 Hz), 36.63, 26.18, 25.89, 18.62, 16.42, $-$4.91. ^{19}F NMR (376 MHz): δ $-$150.31 (m), $-$154.11 (m). IR (KBr): 2120, 1491. LRMS (EI) *m*/*z* (relative intensity): 446 (50%, M^+), 418 (44%, M^+ $-$ N_2), 246 (100%). HRMS calcd for $C_{20}H_{30}F_4N_4OSi$ (M^+), 446.2125; found, 446.2164.

6-(4-Azido-2,3,5,6-tetrafluorobenzyloxy)-1-*tert*-butyldimethylsilyloxy-3-methyl-2-hexene (32). 4-Azido-2,3,5,6-tetrafluorobenzoyl chloride[63] (119 mg, 0.47 mmol) was dissolved in CH_2Cl_2 (1 mL), and pyridine (38 μL, 0.47 mmol) was added. Alcohol **27** (104 mg, 0.42 mmol), dissolved in 4 mL of CH_2Cl_2, was then slowly added. After the reaction was stirred at room temperature overnight, water was added, and the reaction was extracted with hexane. The combined organic layers were washed (1 N HCl, then 5% $NaHCO_3$, then water), dried ($MgSO_4$), filtered, and evaporated to give 180 mg (93%) of **32** as a colorless oil which was used in the next reaction without further purification. An analytical sample was prepared by flash chromatography (2% EtOAc in hexane). ^{1}H NMR (400 MHz): δ 5.37$-$5.33 (m, 1H), 4.36 (t, 2H, J = 6.4 Hz), 4.20 (dd, 2H, J = 6.4 Hz, J = 0.8 Hz), 2.16$-$2.12 (m, 2H), 1.92$-$1.86 (m, 2H), 1.65 (s, 3H), 0.90 (s, 9H), 0.07 (s, 6H). ^{13}C NMR (100 MHz): δ 159.71, 146.92 (m), 144.35 (m), 142.06 (m), 139.56 (m), 135.63, 125.86, 123.56 (m), 108.35 (m), 66.55, 60.55, 35.83, 26.78, 26.35, 18.78, 16.58, $-$4.74. ^{19}F NMR (376 MHz): δ $-$139.94 (m), $-$152.11 (m). IR (KBr): 2120, 1735, 1483. LRMS (EI) *m*/*z* (relative intensity): 461 (12%, M^+), 460 (32%, M $-$ H^+), 433 (100%, M^+ $-$ N_2). HRMS calcd for $C_{16}H_{18}F_4N_3SiO_3$ (M $-$ $C_4H_9^+$), 292.1645; found, 292.1645.

General Halogenation Conditions for Compounds 33 and 35. To a solution of Ph_3PCl_2 (78 mg, 0.23 mmol) in CH_2Cl_2 (0.5 mL) was added the silyl ether (0.10 mmol) dissolved in CH_2Cl_2 (0.75 mL). After being stirred at room temperature for 1.5 h, the reaction mixture was loaded directly onto a silica gel column and purified by flash chromatography (2% EtOAc in hexane) to afford the allylic chloride which was used immediately in the pyrophosphorylation step.

6-Chloro-4-methyl-4-hexene-(4-azidotetrafluorobenzoate) (33). Yield (87%). TLC: R_f 0.54.

***N*-(6-Chloro-4-methyl-4-hexenyl)-*N*-methyl-4-azidotetrafluoroaniline (35).** Yield (87%). TLC: R_f 0.63.

General Pyrophosphorylation Conditions for Compounds 6 and 7. To a solution of the allylic chlorides **33** or **35** (20 mg, 0.06 mmol) in dry acetonitrile (3 mL) was added tris(tetrabutylammonium)hydrogen pyrophosphate (140 mg, 0.16 mmol). The reaction was allowed to stir at room temperature for 4 h. Solvent was removed, and the residue was dissolved in 3 mL of ion-exchange buffer. The resulting milky white solution was loaded onto a cation-exchange resin (NH_4^+ form), eluted with ion-exchange buffer, and the eluant was lyophilized. A portion of the crude pyrophosphate (ca. 25 mg) was dissolved in 1 mL of 25 mM NH_4CO_3. The solution of compound **6** was loaded (in 100 λ portions) onto a Vydac 218TP1010 C_{18} column (250 mm $\times$ 10 mm) monitoring at 254 nm and eluted under the following gradient at a flow rate of 4 mL/min: 0 $\rightarrow$ 6 min 100% A, 6 $\rightarrow$ 18 min 5% A, 18 $\rightarrow$ 19 min 5% A, 19 $\rightarrow$ 24 min 100% A, 24 $\rightarrow$ 35 min 100% A (A = 25 mM NH_4HCO_3, B = CH_3CN). The solution of compound **7** was loaded onto a Western Analytical 250 $\times$ 10 mm, 5 μm BioBasic8 C_8 monitoring at 254 nm and eluted under the following gradient at a flow rate of 4 mL/min: 0 $\rightarrow$ 6 min 95% A, 6 $\rightarrow$ 31 min 5% A, 31 $\rightarrow$ 36 min 5% A, 36 $\rightarrow$ 43 min 95% A, 43 $\rightarrow$ 50 min 95% A (A = 25 mM NH_4HCO_3 in H_2O, B = CH_3CN).

6-(*N*-Methyl-4-azidotetrafluoroaniline)-3-methyl-2-hexene Pyrophosphate (6). Fluffy white solid (40%). t_R: 13.8 min. ^{1}H NMR (D_2O, 400 MHz): δ 5.18 (m, 1H), 4.23 (t, J = 6.8 Hz, 2H), 2.81 (t, J = 7.8 Hz, 2H), 2.61 (s, 3H), 1.82 (t, J = 7.4 Hz), 1.44 (s, 3H), 1.40$-$1.30 (m, 2H). ^{13}C NMR (D_2O, 100 MHz): δ 146.05 (m), 143.54 (m), 142.38, 142.2 (m), 139.8 (m), 125.04 (m), 119.9, 116.09 (m), 62.91 (d, J = 5.3 Hz), 55.61, 41.64, 36.27, 24.77, 15.39. ^{19}F NMR (D_2O, 376 MHz): δ $-$149.54 (m), $-$154.47 (m). ^{31}P NMR (D_2O, 162 MHz): δ 21.19 (d, 1P, J = 20.8 Hz), 20.84 (d, 1P, J = 20.8 Hz). IR (KBr): 2120. LRMS(FAB$^-$, glycerol matrix): (M $-$ H^+) 491, (M $-$ N_2) 464.

6-(4-Azidotetrafluorobenzylester)-3-methyl-2-hexene Pyrophosphate (7). Fluffy white solid (40%). t_R: 17.8 min. ^{1}H NMR (D_2O:CD_3CN 2:1, 400 MHz): 5.46 (m, 1H), 4.50$-$4.30 (m, 4H), 2.19 (m, 2H), 2.01 (m, 2H), 1.72 (s, 3H). ^{13}C NMR (D_2O:CD_3CN 2:1, 125 MHz): 160.92, 146.72 (m), 144.76 (m), 141.97 (m), 140.24 (m), 140.97, 124.43 (m), 121.75, 107.34 (m), 67.23, 63.05, 35.61, 26.69, 16.19. ^{19}F NMR (D_2O:CD_3CN 2:1, 376 MHz): $-$140.76 (m), $-$152.34 (m). ^{31}P NMR (D_2O:CD_3CN 2:1, 202.37 MHz): 10.8 (d, 1P, J = 18.5 Hz), 10.1 (d, 1P, J = 18.5 Hz). IR (KBr): 2128, 1720. LRMS (FAB$^-$, glycerol matrix): (M $-$ H^+) 506, (M $-$ N_2) 479.

General Biological Materials and Methods. [1-^{3}H]-Farnesyl pyrophosphate ([^{3}H]FPP, 15 Ci/mmol) was obtained from American Radiochemical Co. Recombinant Ras-CVLS was produced in bacteria

as described previously.[81] All other solvents and chemicals were reagent grade and purchased from standard commercial sources.

Biochemical Evaluation: Continuous Fluorescence Assay. The kinetic constants K_m, V_{max}, and k_{cat} for FPP and FPP analogues **2**−**4** were determined using the continuous spectrofluorimetric assay as previously described.[37] The peptide *N*-dansyl-GCVLS was synthesized and HPLC-purified by the MSAF facility at the University of Kentucky. Rat protein farnesyltransferase containing a 6X His-tag with a thrombin cleavage site on the N-terminus of the β subunit (N-terminus = MGSSHHHHHHSSGLVPRGSH) was recombinantly expressed in BL21(DE3) *E. coli* cells[82] and purified using a Ni(II)-charged IMAC (immobilized metal affinity chromatography, POROS) column with an imidazole gradient. The purified protein was >90% pure, as judged by SDS−PAGE analysis. Fluorescence was detected using a time-based scan at 30 °C for a period of 60 s.

The kinetic constants K_m, V_{max}, and k_{cat} for FPP and the analogues **2**−**4** were determined using the continuous spectrofluorimetric assay originally developed by Pompliano et al.[74] and modified by Poulter and co-workers[75] with some additional modification. Utilizing *N*-dansyl-GCVLS as the peptide substrate, we measured the linear portion of the increase in fluorescence versus time with a Hitatchi F2000 spectrofluorimeter (excitation wavelength, 350 nm; emission wavelength, 505 nm). The assay components {209.6 μL of assay buffer (50 mM Tris-HCl, pH 7.5, 5 mM DTT, 5 mM $MgCl_2$, 10 μM $ZnCl_2$), 40 μL of detergent solution (0.4% *n*-dodecyl-β-D-maltoside in H_2O), 0.4 μL of *N*-dansyl-GCVLS solution (1 mM in 20 mM Tris-HCl, pH 7.5, 10 mM EDTA), 100 μL of FPP or FPP analogue (2−20 mM stock solutions in 12 mM NH_4HCO_3:MeOH (7:3 v/v); final concentration 0.03−3 μM)} were assembled in a 1.5 mL Eppendorf tube in the order indicated above and incubated at 30 °C for 5 min. A 50 μL FTase solution (0.1 mg/mL BSA with 0.27 μM FTase (for FPP only) or 1.2 μM FTase in assay buffer) was loaded into a 1.0 mL quartz cuvette and incubated at 30 °C for 5 min. The reaction was initiated by the addition of the 350 μL assay buffer/peptide/prenyl pyrophosphate solution to the 50 μL FTase/BSA solution. Fluorescence was detected using a time-based scan at 30 °C for a period of 60 s. The velocity was determined by converting the rate of increase in fluorescence intensity units (FLU/s) to pmol/s by fitting the data to eq 1.

$$V = \frac{R \times P}{\mathrm{FMAX}} \tag{1}$$

V is the velocity of the reaction in pmol/s. *R* is the rate of the reaction in FLU/s. *P* is equal to the number of picomoles of FPP or analogues **2**−**4** used in the reaction mixture when the number of *N*-dansyl-GCVLS picomoles is 2-fold or greater to the number of prenyl pyrophosphate picomoles. FMAX is the fluorescence intensity of the reaction mixture after incubation for 60 min at 30 °C when an amount of P was used for FPP or analogues **2**−**4**. On the basis of HPLC analysis of large-scale reactions under similar conditions, we assume that each reaction has gone to completion.

Product Studies. Large-scale reactions contained 50 mM Tris·HCl, pH 7.5, 5 mM $MgCl_2$, 10 μM $ZnCl_2$, 5 mM DTT, 0.04% *n*-dodecyl-β-D-maltoside, 2.5 μM *N*-dansyl-GCVLS, 0.25 μM FTase, and 25 μM FPP or **2**−**6** in a final reaction volume of 400 μL. After the samples were allowed to react for 1 h at 37 °C, each reaction mixture was loaded onto an analytical Vydac C_8 (208TP54) column and eluted with a linear gradient of 0−40 min 10% B to 100% B at a flow rate of 1 mL/min. Solvents: A = 0.01% (v/v) TFA in water; B = 0.01% (v/v) TFA in CH_3CN. The fraction corresponding to coincident absorbance and fluorescence peaks was collected and analyzed by mass spectroscopy.

***N*-Dansyl-G-(farnesyl-1-*S*-cysteine)-VLS (43).** HRMS (ESI): calculated for $C_{46}H_{71}N_6O_9S_2$, 915.4724; measured, 915.4726.

***N*-Dansyl-G-(8-anilinogeranyl-1-*S*-cysteine)-VLS (44).** HRMS (ESI): calculated for $C_{47}H_{68}N_7O_9S_2$, 938.4520; measured, 938.4568.

***N*-Dansyl-G-(8-pentafluoroanilinogeranyl-1-*S*-cysteine)-VLS (45).** HRMS (ESI): calculated for $C_{47}H_{63}F_5N_7O_9S_2$, 1028.4049; measured, 1028.4029.

***N*-Dansyl-G-(8-(*p*-nitroanilino)geranyl-1-*S*-cysteine)-VLS (46).** HRMS (ESI): calculated for $C_{47}H_{67}N_8O_{11}S_2$, 983.4371; measured, 983.4373.

***N*-Dansyl-G-(8-(*N*-ethyl-*p*-azidotetrafluoroanilino)geranyl-1-*S*-cysteine)-VLS (47).** LRMS (ESI): calculated for $C_{49}H_{68}F_4N_{10}O_9S_2$, 1080.4993; measured, 1079.62. HRMS ($-N_2 + H$ = 1053.5010, measured, 1053.5016) ($-N_2 + 2H$ = 1054.5088), measured, 1054.5050 ($-N_2 + 2H$).

***N*-Dansyl-G-(6-(*N*-methyl-*p*-azidotetrafluoroanlino)-3-methyl-2-hexenyl-1-*S*-cysteine)-VLS (48).** HRMS (ESI): calculated for $C_{45}H_{62}F_4N_{10}O_9S_2$, 1026.4079 ($-N_2 + H$ = 999.4095, measured 999.4081) ($-N_2 + 2H$ = 1000.4174), measured, 1000.4118 ($-N_2 + 2H$).

***N*-Biotin-G-(8-(*N*-ethyl-*p*-azidotetrafluoroanilino)geranyl-1-*S*-cysteine)-VLS (49).** HRMS (ESI): calculated for $C_{47}H_{69}F_4N_{11}O_9S_2$, 1071.4657; measured, 1071.5.

Photoinactivation of FTase. Farnesyltransferase activity was assayed by measuring the amount of [^{3}H]farnesyl transferred from [^{3}H]-FPP to recombinant Ras, as described previously.[83] Unless otherwise stated, each reaction mixture contained the following components in a final volume of 25 μL: 50 mM Tris (pH 7.4), 20 mM KCl, 10−20 ng of recombinant FTase, 3 mM $MgCl_2$, 50 μM $ZnCl_2$, and 0.6 μM ETAZ-AGPP. The solution was placed underneath a 254 nm hand-held light source (UVP Model UVG-11) and photolyzed for 30 min at 0 °C. After photolysis, a solution of 1 mM dithiothreitol, 5 μM Ras, 0.2% octyl β-glucopyranoside, and 0.6 μM [^{3}H]FPP (33 000 dpm/pmol; American Radiochemical Co.) was added, and the reaction was incubated for 30 min at 37 °C. The amount of [^{3}H]farnesyl transferred was measured by ethanol−HCl precipitation and filtration on glass fiber filters with modification as previously described.[81] A blank value was determined in parallel incubation mixtures containing no enzyme. This blank value was subtracted from each reaction before calculating the picomoles of [^{3}H]prenyl transferred.

pK_a Prediction. We utilized the Hammett eq 2 to describe the pK_a value of an unsubstituted base[84]

$$\mathrm{p}K_a = \mathrm{p}K_a^0 - \rho(\sum\sigma) \tag{2}$$

where pK_a^0 is the pK_a of the unsubstituted base, σ is a constant assigned to a particular substituent, and ρ is a constant for a particular equilibrium. Equation 3 describes the expression for the ionization of substituted anilines at 25 °C[84] (Table A.3):

$$\mathrm{p}K_a = 4.58 - 2.88\sum\sigma \tag{3}$$

A pK_a for pentafluoroaniline was estimated with eq 2 using literature values of σ_{meta} (0.34),[85] σ_{para} (0.06),[85] and apparent σ_{ortho} (0.47)[84] (Table A.5) for fluorine. The pK_a for 4-azidotetrafluoroaniline was then estimated with eq 2 when the literature values for σ_{meta} (0.34) and apparent σ_{ortho} (0.47) for fluorine were used, along with a σ_{para} (0.15)[85] value for azide.

$$\mathrm{p}K_a = 4.85 - \rho\sum\sigma \tag{4}$$

Equation 4 describes the expression for the ionization of substituted *N*-methyl anilines. To determine the pK_a of *N*-methyl-4-azidotetrafluoroaniline, we first fit the literature pK_a value for *N*-methyl-pentafluoro-

(81) Crick, D. C.; Suders, J.; Kluthe, C. M.; Andres, D. A.; Waechter, C. J. *J. Neurochem.* **1995**, *65*, 1365−1373.
(82) Zimmerman, K. K.; Scholten, J. D.; Huang, C.-C.; Fierke, C. A.; Hupe, D. J. *Protein Expression Purif.* **1998**, *14*, 395−402.
(83) Andres, D. A.; Goldstein, J. L.; Ho, Y. K.; Brown, M. S. *J. Biol. Chem.* **1993**, *268*, 1383−1390.
(84) Perrin, D. D.; Dempsey, B.; Serjeant, E. P. *pK_a Prediction for Organic Acids and Bases*; Chapman and Hall: London, 1981.
(85) Hansch, C.; Leo, A.; Unger, S. H.; Kim, K. H.; Nikaitani, D.; Lien, E. J. *J. Med. Chem.* **1973**, *16*, 1207−1216.

aniline (0.676 ± 0.012)[72] to eq 3 along with the σ values used above for pentafluoraniline to determine ρ. The pK_a value for *N*-methyl-4-azidotetrafluoroaniline was then estimated with eq 3 when the σ values used above for 4-azidotetrafluoroaniline were employed.

Molecular Modeling. The FTase starting structure was created by adding hydrogen atoms to the binary FTase-FPP crystal structure structure (PDB code 1FT2). Atom potential types and partial charges were assigned on the basis of the cff91 force field defaults. The cysteine and histidine residues coordinating the zinc atom were considered to be deprotonated, and their charges were modified accordingly. Because charges for the deprotonated residues are not provided in the cff91 force field library, charges for deprotonated cysteine were taken from the AMBER 6.0 library, charges for deprotonated histidine (histidinate) were taken from Pang et al.[86] FPP, and analogue starting structures were constructed in the "Builder" module of Insight II (v2000, MSI, Inc.). The optimal geometery and atomic charges of the termini of the analogues were calculated using density functional methods (SVWN) as implemented in MacSpartan Pro. The DN* basis set and SCF damping (0.5) were used. The atomic charges of the remainder of the analogues were assigned on the basis of RESP fitting of FPP. Atom potential types were assigned automatically on the basis of hybridization and connectivities.

All ligand starting structures were in the fully extended conformation. Analogues **5** and **6** were modeled in both cis and trans conformations with respect to the relative orientation of the azido group and main chain about the aniline C−N bond. Minimization and molecular dynamics were set up using the "Docking" module and carried out with the "CDiscover" module of Insight II (v2000, MSI, Inc.) under the cff91 force field. Optimal geometry in the analogue termini was enforced by angle and torsional restraints. The coordinates of all protein residues were fixed, except for the following active site residues, which were allowed to move: Tyr 200α, His 201α, Trp 102β, Ala 151β, Tyr 154β, Met 193β, Asp 200β, Arg 202β, Tyr 205β, Cys 206β, Gly 250β, Tyr 251β, Phe 253β, Cys 254β, Trp 303β, Tyr 361β, Tyr 365β. A two-stage refinement was used to model the binary complexes. The first round consisted of a Monte Carlo conformational search and minimization, from which 50 structures were generated. This was done with the electrostatic component of the force field turned off and the van der Waals component scaled to 10%. The second round consisted of a Monte Carlo conformational search and minimization of the 50 generated structures with all components of the force field at 100% and inclusion of a distance-dependent dielectric component (dielectric constant = 1) followed by simulated annealing consisting of 50 increments of 100 fs each to cool the system from 500 to 300 K. The overall and per residue binding energy of each of the final 50 structures were then measured via a CDiscover routine. For comparison to these generated structures, the modified 1FT2 binary cocrystal structure was also minimized as in the second round of refinement (without simulated annealing), and the FTase-FPP binding energy was calculated.

Acknowledgment. We thank Mark Meier for assistance with MacSpartan, Robert Dickson and Robert Lester for assistance with the HPLC fluorescence analysis, and Louis Hersh for his advice with the enzyme kinetics. This work was supported in part by the American Heart Association grant (to D.A.A.), the National Science Foundation grant MCB-9808633 (to H.P.S.), the Kentucky Lung Cancer Research Program (to H.P.S. and D.A.A.), Kentucky-NSF EPSCoR Program (EPS-9452895) (to H.P.S.), and the National Institutes of Health (GM40602 to C.A.F.).

Supporting Information Available: ^{1}H, ^{13}C, ^{31}P, ^{19}F NMR, IR, and MS spectra as appropriate are available for compounds reported (PDF). This material is available free of charge via the Internet at http://pubs.acs.org.

JA0124717

(86) Pang, Y.-P.; Xu, K.; El Yazal, J.; Prendergast, F. G. *Protein Sci.* **2000**, *9*, 1857−1865.